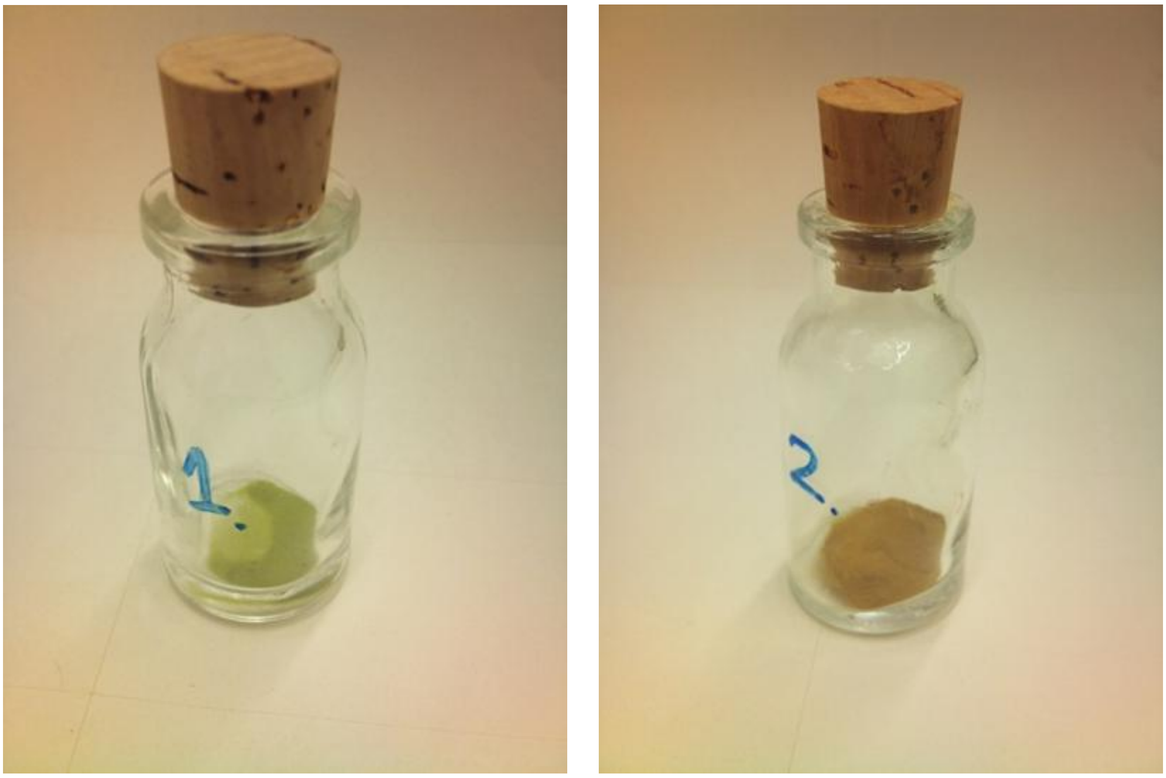

Catalytic Partial Oxidation of Methane over $Fe_2(MoO_4)_3$ Catalysts

Master’s Thesis in Materials and Nanotechnology Programme

DAZHENG JING

Department of Chemical and Biological Engineering
Division of Applied Surface Chemistry and Competence Centre for Catalysis
CHALMERS UNIVERSITY OF TECHNOLOGY
Göteborg, Sweden 2010
Master’s Thesis 2010

MASTER’S THESIS 2010

Catalytic Partial Oxidation of Methane over $Fe_2(MoO_4)_3$ Catalysts

Master’s Thesis in Materials and Nanotechnology Programme

DAZHENG JING

Examiner: Prof. Magnus Skoglundh

Supervisor: Assist. Prof. Per-Anders Carlsson

Department of Chemical and Biological Engineering
Division of Applied Surface Chemistry and Competence Centre for Catalysis
CHALMERS UNIVERSITY OF TECHNOLOGY

Göteborg, Sweden 2010

Catalytic partial oxidation of methane over $Fe_2(MoO_4)_3$ catalysts
Master's Thesis in Materials and Nanotechnology Programme
DAZHENG JING

Master's Thesis 2010

Department of Chemical and Biological Engineering
Division of Applied Surface Chemistry and Competence Centre for Catalysis
Chalmers University of Technology
SE-412 96 Göteborg
Sweden
Telephone: + 46 (0)31-772 1000

Cover:
Potential catalysts for methanol production from methane. The left panel (sample 1) shows the $Fe_2(MoO_4)_3$ powder catalyst synthesized in a solution with pH=1.65 and the right panel (sample 2) is the corresponding catalyst synthesized at pH=3.

Göteborg, Sweden 2010

Catalytic partial oxidation of methane over $Fe_2(MoO_4)_3$ catalysts
Master's Thesis in the Materials and Nanotechnology Programme
DAZHENG JING
Department of Chemical and Biological Engineering
Division of Applied Surface Chemistry and Competence Centre for Catalysis
Chalmers University of Technology

ABSTRACT

The study of new energy carriers for sustainable energy conversion processes is a hot research area. Among the potential energy carriers one finds biogas, containing a large fraction of methane, which attracts high interests worldwide. However, to be more useful, e.g., concerning storage and transportation, conversion of gaseous methane fuel into liquid fuel like methanol is desired. The conventional route for production of methanol from methane is a two-step process including energy intensive syngas production. To reduce energy costs, direct catalytic conversion of methane to methanol provides an attractive possibility to circumvent syngas production provided proper catalysts can be found.

In this work, $Fe_2(MoO_4)_3$ catalysts were hydrothermally synthesized and tested as potential methanol production catalysts. By employing different pH value of the precursor solution different catalysts were formed, i.e., pale green (pH=1.65) and brown (pH=3) colored iron molybdate samples. Transient (pulse-response) methane oxidation experiments were performed in a continuous gas-flow reactor connected with a mass spectrometer. Essentially five parameters were studied: i) reaction temperature, ii) catalyst preparation route, iii) CH_4/O_2 ratio iv) H_2 addition and v) the concentration of hydrogen. Analysis of BET surface area and XRD patterns for fresh and treated samples was performed as well.

The pulse-response experiments show that the reaction is promoted by high temperature and also is very sensitive to the reactant composition. Addition of hydrogen shifts the product selectivity to some extent. Both samples seem to have the ability to store and release oxygen during lean/rich cycling. The study shows that methanol may be produced in small amounts for certain reaction conditions.

Key words: Sustainable energy carrier, methane partial oxidation, methanol, $Fe_2(MoO_4)_3$ catalyst

Contents

1 Introduction

1.1 Project background

The increased usage of petroleum in the modern society together with decreasing resources of crude oil accentuates the need to find alternative energy carriers to fossil based oil for energy conversion processes. Moreover, concerns about climate change related to enhancement of global warming due to emissions of greenhouse gases are increasing. All together this stimulates the worldwide R&D on finding new sustainable energy conversion processes. Among the renewable sources often discussed one finds solar-, wind-and water energy. Also various processes relying on the utilization of a biological feedstock are discussed. In this connection, to be efficiently used, transformation of biomass into other energy carriers like biogas and biodiesel, alcohols and ethers are considered. In this project, partial oxidation methane (CH_4) over heterogeneous catalysts for potential production of methanol (CH_3OH) is considered.

Biogas refers to the gas produced from biomass in the absence of oxygen. The raw materials in biogas production include organic waste, manure, sewage, municipal waste and even animal dung. The production of biogas is environmentally friendly as otherwise useless waste is converted to a usable energy carrier. Additionally, the residuals may serve as useful fertilizers. Methane and carbon dioxide are the main constituents of biogas accounting for, respectively, 65 and 30 vol. % [1].

Biogas (and associated derivatives) is a carbon neutral fuel. Thus conversion of biogas by, for example, oxidation into water and carbon dioxide, will not contribute to the increase of the (average) concentration of carbon dioxide in the atmosphere [2]. The carbon balance is fulfilled as long as carbon neutral fuels are used. For example, hypothetically, one mole of atmospheric CO_2 is required to produce one mole of methanol that after burning, in an energy conversion process again, forms one mole of CO_2 emitted to the atmosphere. Here, methanol acts as an energy carrier in this “one carbon in - one carbon out” process without bringing any other effects.

As most of the facilities for production of biogas are located in remote areas, transportation of biogas is an essential issue that may be connected with significant energy costs and safety risks. In case of vehicle transportation, high-pressure cylinders are required to carry sufficient quantities. This is, however, associated with high explosion risks. To decrease the potential risk of explosion, heavy gas containers with thick walls are needed. Such containers demands extra material and may lead to even more severe damages in case of explosion. For this reason, liquid fuels are preferred. In addition to safety aspects, liquid fuels contain more energy per unit volume thanks to the high density of the condensed phase. Transportation of liquid fuels is thus beneficial, as compared to gaseous fuels, and conforms better to sustainable transports.

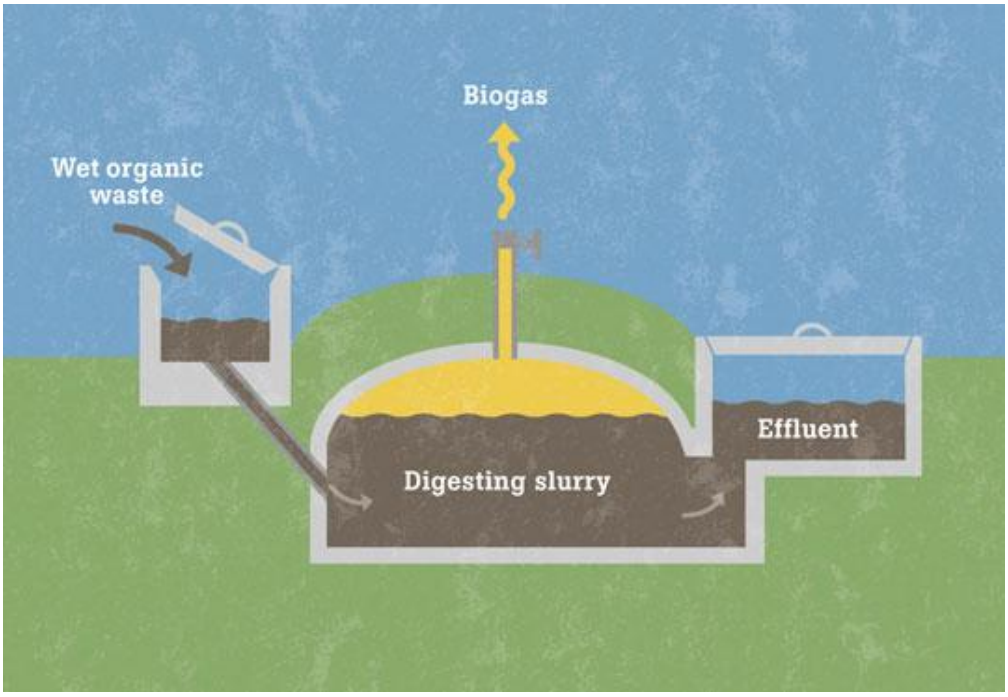

Figure 1.1 Schematic of a fixed dome plant commonly used for small-scale production of biogas. The raw material (wet organic waste) is fed into a reservoir from where it falls into the reactor dome constituting both slurry- and gas containers. Bacteria in the raw material digest the slurry so as to produce biogas leaving at the top [3].

Conversion of methane into liquid methanol has attracted attention by researchers both in industry and academia. The conventional route to produce methanol is a two-step process via an intermediate CO/H_2 gas mixture, so-called synthesis gas or syngas. The production of syngas is often based on a three-step process involving i) stream reforming, ii) carbon dioxide (or dry) reforming and iii) partial oxidation [4]. Steam reforming of methane is an energy intensive process that requires high temperature and pressure. The process is carried out in large furnaces. The necessary high temperature put strong demands on issues like process operation, reactor construction and maintenance. Steam reforming is an expensive process. For example, the costs associated with steam reforming in syngas generation in processes for conversion of CH_4 to methanol, production of ammonia and Fischer-Tropsch products has been estimated be over 60% of the overall process cost [5].

With the aim to circumvent the high energy demands and associated costs in the two-step process for production of methanol, direct conversion of methane to methanol by catalytic partial oxidation attracts great interests. Large efforts on finding appropriate catalysts that can realize this one-step process have been made. During the last two decades, a significant number of studies on various catalysts have been reported. Despite this, attractive processes are still lacking as the present catalytic processes suffer from low yields of methanol and thus has a low commercial viability [6].

1.2 Project objective

The objective of the present master thesis is to i) screen the open literature to document typical catalyst formulations and catalytic processes for conversion of methane into methanol and ii) study partial oxidation of CH_4 over $Fe_2(MoO_3)_4$ as a potential catalyst for production of methanol (CH_3OH).

2 Catalytic conversion of methane into methanol

2.1 Concepts in heterogeneous catalysis

Historically, catalysis as a phenomenon was coined first by J. J. Berzelius:

> *"Many bodies have the property of exerting on other bodies an action which is very different from chemical affinity. By means of this action they produce decomposition in bodies, and form new compounds into the composition of which they do not enter. This new power, hitherto unknown, I shall call it catalytic power. I shall also call catalysis the decomposition of bodies by this force [7]."*

Catalysis is the change of chemical reaction rate when a small amount of a material, called catalyst, is added. Unlike reactants, a catalyst itself is not consumed during a reaction. A catalyst can only influence thermodynamically possible reactions. It augments a reaction rate by changing the apparent activation energy of the reaction by providing new reaction routes. Catalysis is commonly categorized into three different cases, i.e., homogeneous catalysis, heterogeneous catalysis and enzymatic catalysis. The feature of homogeneous catalysis is that the catalyst and reactants are contained in the same phase. In heterogeneous catalysis, the catalyst (usually a solid) and the reactants (gases or liquids) are present in different phases. For enzymatic catalysis, protein is the catalyst [8].

Heterogeneous catalysis is one of the most important technologies for our modern society. It underpins the chemical and materials industries, being fundamental to the production of fuels and solving pollution problems [9]. The heterogeneous catalytic cycle is commonly described by the five steps. Here we demonstrate these steps by using the example CO oxidation on a supported metal see Fig.2.1. The first step is the diffusion of gas phase CO and O2 to the metal surface. The second step involves the associative (molecular) adsorption of CO and dissociative (molecule splitting) adsorption of O2 on the metal surface. These adsorption events are so-called chemisorption processes where new chemical bonds are formed to be separated with physisorption for which molecules interacts more weekly with the surface. The third step is the surface reaction between CO and O (this step also involves surface diffusion of reactants and products). The desorption of the formed product CO2 is the fourth step and finally the fifth step is the diffusion of CO2 to the gas phase. Fig.2.2 and Fig.2.3 show the energy diagrams of adsorption and catalytic cycle in heterogeneous catalysis.

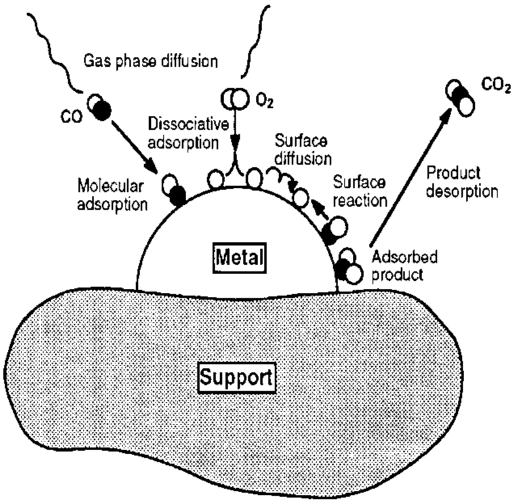

Fig. 2.1 Schematic present of stages of a heterogeneous catalysis reaction[8]

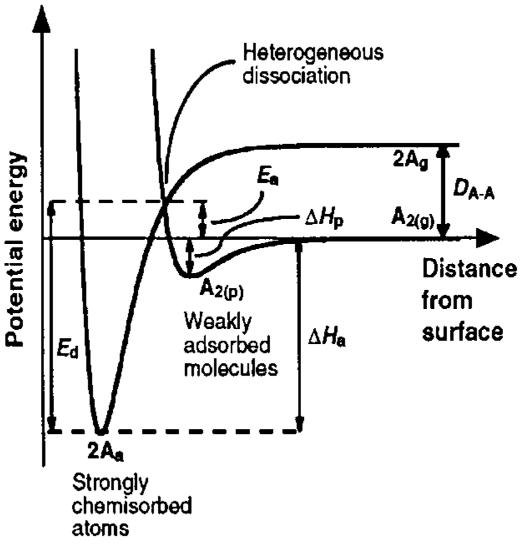

Fig. 2.2 Energy diagram of adsorption on a catalyst surface[8]

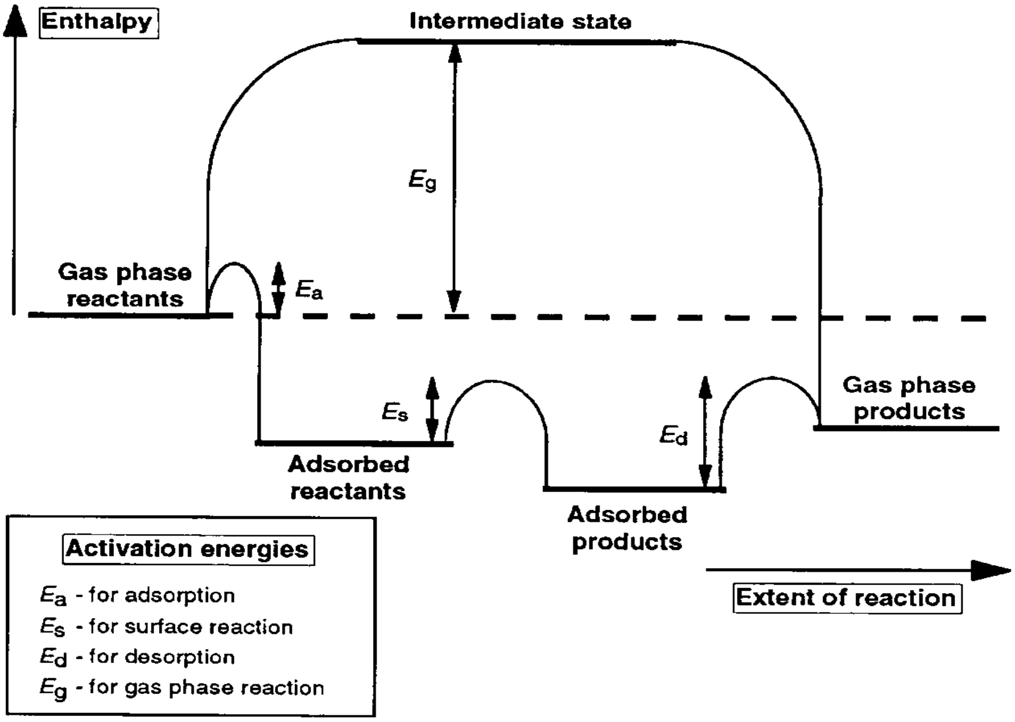

Fig. 2.3 Energy diagram of a heterogeneous reaction [8]

2.2 Properties of methane

Methane (CH_4) is the first compound in the alkane series. The melting- and boiling point is, respectively, -182.5 and -161.5 °C. Methane is a symmetric molecule with no functional group, magnetic moment or polar distribution that can facilitate chemical attacks and thus methane is very stable. The C-H bond is strong reflected by the high dissociation energy of CH_3-H bond (439.3 kJ/mol). Activation of CH_4 by splitting a first C-H bond requires high temperatures and/or the use of strong oxidation agents [10]. Concerning the transformation of methane into other partially oxidized products like CO and methanol is thus a dilemma, as the activation of methane most often requires temperatures too high to avoid complete oxidation. For this reason, the basic concept of direct catalytic partial oxidation of methane into methanol is to find a catalyst that can activate methane under mild conditions while simultaneously preserve formed methanol.

2.3 Processes for converting methane to methanol

The partial oxidation of methane in gas phase occurring at high pressure is dominated by free radical reactions. Thus the presence of solid catalyst cannot change significantly those reactions. However, at lower pressures, around 1 atm, which is preferred in industrial processes, the inclusion of catalysts plays an essential role for both product yield and selectivity [10].

Homogeneous catalysis

Among the homogeneous catalytic processes for conversion of methane to methanol, mercury-catalyzed reactions for high yield of methyl bisulfate as a pre-product for methanol production have been proposed. The reaction occurs in concentrated sulfuric acid under mild conditions (180 °C). The catalyzed oxidation of methane by mercuric ions is remarkable efficient. For a 50% methane conversion a 85% selectivity to methyl bisulfate (43% yield) have been reported [11]. A drawback, however, is that this is a two-step process including separation and hydrolysis of methyl bisulfate and re-oxidation of sulfur dioxide, which may be difficult and expensive to handle in industrial production.

An alternative of the mercury based system is the route including a bipyrimidylplatinum (II) complex. Using this Pt complex, 90% conversion of methane into methyl bisulfate at 493K and 35bar with selectivity of 81% has been reported. It is expected that methyl bisulfate can be hydrolyzed to methanol in later step. Although both high conversion and selectivity to intermediates are achieved the complete production cycle demands an expensive process step where the catalyst is regenerated from the concentrated sulfuric acid. Also the high pressure is not preferred in industry. All in all, the two-step homogeneous catalytic process described here are not sufficiently attractive for methanol production [12].

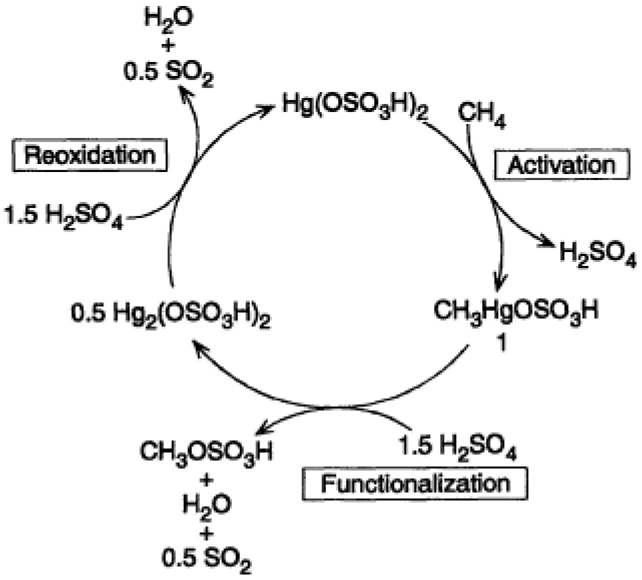

Fig. 2.4 The suggested working model for mercury-catalyzed methane reactions [11]

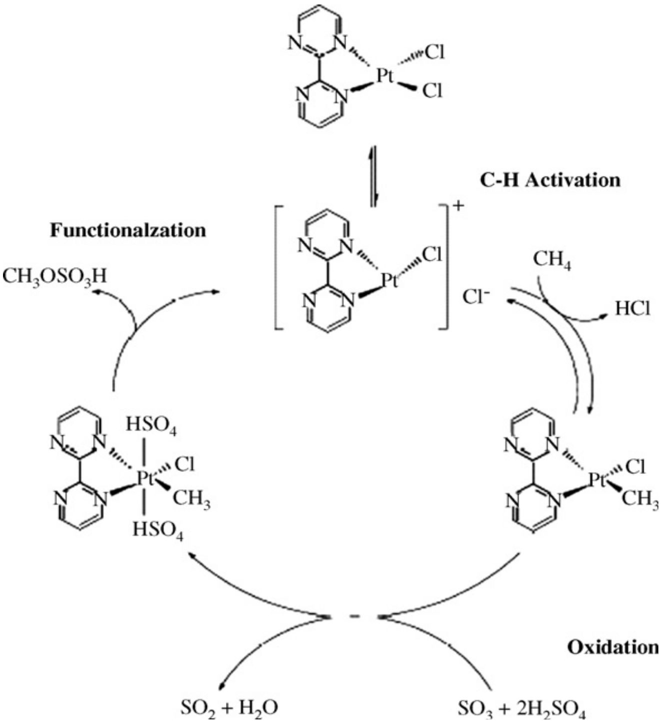

Fig.2.5 Reaction mechanism for methane partial oxidation using a bipyrimidylPt(II) complex in concentrated sulfuric acid [12].

Plasma processes and doping effects

The influence of applying low-temperature plasma though a dielectric-barrier discharge (DBD) with a $Cu/ZnO/Al_2O_3$ (CZA) based catalyst used for methane conversion have been studied by A. Indarto *et al*. By preparing a CZA catalyst with and without DBD plasma treatment, different types of Cu species in the CZA catalyst are formed. For one of the forms, the selectivity to methanol in the range of 19-23% was observed while for the other form of Cu, the selectivity was around 15-18% under actual experimental conditions. Through sample characterization, Cu^+ and Cu^{2+} were suggested to be the active sites for methane partial oxidation to methanol in low-temperature plasma process [13].In addition to the low- temperature plasma treatment, the influence of doping CZA systems with other elements has also been studied. For example, dopants like Pt, Ni, Fe and Y have been evaluated. Doping CZA with 3 wt.-% Y increases the methanol selectivity from 12% to 31%, which is the largest effect reported for the mentioned dopants [14].

Y. Yamada and co-workers doped silica with 43 different elements and studied the resulting performance in methane partial oxidation. Based on their results, they suggested that V, Fe, Sc, W, Mo and Os are the most suitable elements for improvement of the selective oxidation methane at pressures under 1 atm using O_2 as an oxidant [15].

Furthermore, $MoO_x/La\text{-}Co\text{-}O$ and MoO_x/ZrO_2 have been investigated in methanol production from methane partial oxidation. It was found that 7% (n%) $MoO_x/La\text{-}Co\text{-}O$ resulted in the highest methanol selectivity, i.e., 60% at 420 ℃ and 4.2MPa. The methane conversion was 11.2% and methanol yield was 6.7% in this study [16].

Zeolites like ZSM catalysts are also interesting candidate materials for partial oxidation of methane to methanol. The ZSM-5 molecular sieves with inclusion of iron in a silicon framework were employed as catalysts under atmospheric pressure conditions. Using oxygen as oxidant, both Fe-NaZSM(5) and Fe-HZSM-(5) can produce methanol. Moreover it is found that a certain content of Na in molecular sieves can increase the selectivity towards methanol significantly [17].

K.Otsuka, Y.Wang tested Mo, V_2O_5, MoSnP on SiO_2 supports and blank SiO_2 for partial oxidation of methane [18]. Experiments were carried out in the temperature range 500-650 ℃. Here, HCHO is the main oxidation product with selectivity around 30% depending on the specific catalyst. The highest selectivity towards HCHO is 64.8% with a methane conversion of 7.2%, which is observed for $MoSnP/SiO_2$.

Homogenous additive effects

Homogenous additives H_2, N_2O or NO can enhance methanol selectivity [19, 20]. By introducing small amount of NO into CH_4/O_2 reactants on low surface area V_2O_5/SiO_4, both CH_4 conversion and $HCHO/CH_3OH$ yield are strongly enhanced. Selectivity to C_1-oxygenates can reach 16% at highest at methane conversion close to 40%. Radical initiator NO can circumvent the antagonistic effects in some extend could be the explanation for the improvement [21].

Table 2.1 The effect of N_2O on catalytic proprieties [22]

Catalysts	Temp (℃)	Conversion (%)	Selectivity(%)				
			CO	CO_2	HCHO	CH_3OH	HCHO+CH_3OH
$PMo_{11}V$	700	2	---	77.27	---	22.73	22.73
	750	6	15.58	60.30	5.45	16.67	22.12
$PMo_{11}Fe$	700	2	16.42	52.24	---	31.34	31.34
	750	8	43.26	20.88	13.72	22.14	35.86
$SiMo_{11}Fe$	700	6	46.35	20.76	10.30	22.59	32.89
	750	13	43.29	19.75	21.08	15.88	36.96

Table 2.2 The effect of O_2 on catalytic proprieties [22]

Catalysts	Temp (℃)	Conversion (%)	Selectivity(%)				
			CO	CO_2	HCHO	CH_3OH	HCHO+CH_3OH
$PMo_{11}V$	700	3	43.54	40.90	7.28	19.89	27.17
	750	13	45.86	45.04	15.64	12.25	27.89
$PMo_{11}Fe$	700	4	43.54	19.86	12.92	23.68	36.60
	750	23	45.86	17.42	26.08	10.64	36.72
$SiMo_{11}Fe$	700	4	23.19	47.13	8.23	21.45	29.68
	750	32	27.85	43.84	20.46	7.85	28.31

Heteropolycompound catalysts have been tested using N_2O or O_2 as oxidants under atmosphere pressure. Results presented in the tables below show that selectivity to CH_3OH decreases clearly when temperature increases, whereas both methane conversion and selectivity to HCHO increase. The results from this study support the suggested mechanism where methane is initially oxidized to methanol and then further oxidized to formaldehyde, CO or CO_2, which are more stable oxides [22].

NO significantly promotes the CH_3OH formation using a CH_4/O_2 mixture. On a low surface area V_2O_5/SiO_2 catalyst, 0.39 n% of NO leads to a highest yield, around 7%, of CH_3OH respecting of 27% selectivity under 15% conversion of CH_4. With increasing CH_4 conversion, CH_3OH selectivity reaches a maximum (~27%) at 15%

CH_4 conversion and then diminishes as CH_4 conversion increases. Unfortunately, the concentrations of CH_4 and O_2 are not explicitly accounted for in the article. To avoid decomposition and further oxidation of formed methanol, the downstream temperature is suggested to be an important parameter in experimental studies on the methanol formation process [23].

On $Fe_2(MoO_4)_3$ under atmospheric pressure, main products switched from HCHO and CO to C_2H_6 and C_2H_4 when oxidant O_2 was replaced by N_2O. In O_2 case, it indicates that CH_3OH is the main first step product. However, in the case of N_2O, the concentration of active oxygen species is not high enough to oxidize all CH_3 species to oxygenates, so CH_3 coupling takes place giving C_2H_6 as main products [24]. Mix O_2 with N_2O in order to decrease active oxygen species on catalyst's surface could be useful to prevent methanol further oxidized.

Besides converting methane to methanol, methanol stability over different solid metal catalysts is concerned at the same time. Results show that CeO_2, Fe_2O_3, V_2O_5 convert 30% of methanol at temperature around 300 ℃. WO_3 shows a better result, over which CH_3OH conversion is around 25% at 400 ℃. Sb_2O_3 gives best result during all 33 tested simple oxides. Methanol conversion is as low as 5% around temp 500 ℃, even lower for lower temperature. All the tests are operated under atmosphere pressure. MoO_3, Nb_2O_5, Sb_2O_3, Ta_2O_5 and WO_3 are suggested for methane partial oxidation due to lower methanol decomposition. If contact time can be decreased, formaldehyde is prevented to form hopefully. Injection water may quench gas-phase reaction [25]. These two precautions may assist preserve methanol on catalysts.

Injection of Br_2 into reaction chamber can also improve methanol production. On HgO/ Zn-MCM-41 catalyst, CH_3OH selectivity is increased to 30% at 10% CH_4 conversion after Br_2 injection. The reaction is carried under 1 atm at 220 ℃, reactants mole ration is $CH_4/O_2/Ar$ =3:1:6 [26].

2.4 Mechanistic interpretations

Despite the large efforts reviewed above the encouraging experimental results are still lacking. For the studied catalytic systems either a high methanol selectivity or methane conversion is achieved. Some studies showed excited methanol selectivity together with relative high methane conversions, however, the necessary experimental conditions including high pressure and costly regeneration of condensed sulfuric acid limit the industrial applications.

In order to gain understanding on why methanol production from the reaction between methane and oxygen is so difficult on most solid catalysts, K. Otsuka et al. investigated methane partial oxidation reaction mechanism on $Fe_2(MoO_4)_3$ catalysts. Based on their detailed kinetic measurements and isotopic studies, the authors proposed the reaction scheme is given below. This mechanism is essentially the same for Fe-Nb-B mixed oxide catalyst and similar to silica supported MoO_3 and V_2O_5. It also coincides with mechanisms advised by other scholars on several metal catalysts.

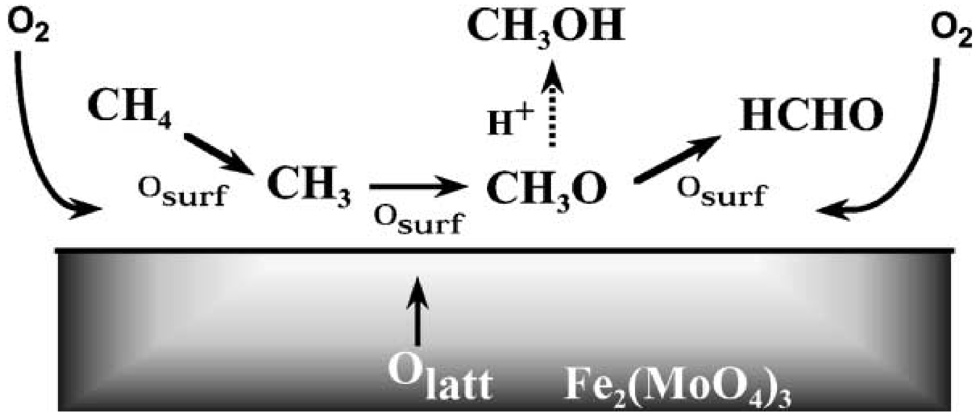

Fig. 2.6 Schematic reaction model for the partial oxidation of methane on the surface of iron molybdate catalyst [27]

Activated surface oxygen species from either dissociative adsorption of gaseous oxygen or diffusion of bulk lattice oxygen from the $Fe_2(MoO_4)_3$ may promote methane dissociation into CH_3 which can react further CH_3O. Both CH_3 and CH_3O are considered to be reaction intermediates. If proton is offered, CH_3OH can be produced from the intermediate CH_3O. Most of the intermediate species would be further attacked by surface oxygen giving products HCHO or CO_X. Aiming at high selectivity of methanol, special structure catalysts which can provide both Brönsted acid active sites for protonation and protect intermediate from further oxidation to HCHO or CO_X are recommended. However, such bifunctional catalysts working well under experimental conditions are still to be found. However, it offers a conceptual direction for selective synthesis of methanol from partial oxidation of methane. Also catalytic processes that can occur at low temperatures is important, as CH_3OH otherwise may decompose on the $Fe_2(MoO_4)_3$ surface (> 500 ℃) [27].

Based on a kinetic study on Pd/Al_2O_3, the first step of activating CH_4 needs an easy H acceptor. Then a good proton donor is favorable to have a high CH_3OH selectivity. Low oxidant concentration is preferred to prevent further oxidation of methane to formaldehyde, CO or CO_2. One option for an improved reaction process may be to transiently switch on and off O_2 while keep CH_4 concentration at a certain level. To produce some CH_3OH, hydrogen peroxide, donating H^+ easily, can be considered to add to gas mixture. H_2O is suggested to be a good option to decrease formaldehyde synthesis [28, 29].

A specific iron phosphate attracts scholars' interest. The uniqueness of this structure is that iron atoms are coordinated tetrahedrically and are isolated by phosphate groups. As the iron sites are considered to be responsible for the (partial) oxidation of methane, isolating adjacent active sites from each other is expected to decrease the risk of further oxidation into unwanted side products. A proposed mechanism is shown in Fig. 2.7 H_2-O_2 and CH_4 are reactants.

In a suggested mechanism, surrounding phosphate groups are bifunctional acting both as proton accepters and proton donors, and probably enhance H_2O_2 formation. At first, phosphates groups accept protons from H_2, forming O-O groups together with iron sites (steps B, C and D). The formed H_2O_2 groups at isolated Fe sites are protected from H_2 attacking which is adsorbed on the most neighboring iron sites. Then O-O groups activates methane (step E) and produce intermediate CH_3O. CH_3OH is produced by CH_3O obtaining a proton from neighboring phosphate group (step F). Acidic protons formed at phosphate groups would promote the CH_3O protonation to form CH_3OH.The isolated Fe sites also protect formed CH_3O or CH_3OH adsorbed on the site from attack of O_2 on the most neighboring sites [18]. Step E is the hardest. It calls for a rapid protonation, while no further oxidation happens.

By studying the selective oxidation of methane to formaldehyde, Dowden et al. suggested approaches for designing novel catalysts [30]. To obtain considerable amount of selective products HCHO and CH_3OH, one vital job is to suppress the total oxidation of products. Theoretically, a perfect catalyst for methane partial oxidation should have dehydrogenation, oxygen insertion as well as hydration capabilities. When methane is attached to a catalyst surface, dehydration of methane produces two major intermediates, CH_3 and CH_2. They are chemisorbed on the catalyst's surface. In order to inhibit total oxidation, the dehydration of intermediates methyl or methylene should be suppressed considering their migration. Methylene groups bond to metal surface more firmly than methyl groups, leading that they are more susceptible to further dehydrogenation. Therefore, the formation of intermediate methyl is preferred. This indicates that an oxides catalyst is more suitable than metal, which can prevent forming CH_2. Mo and V oxides are suggested. Another suggestion is the bond strength of CH_3 to the surface should be weaker than the one of O_2 to the surface. In this case methyl migration is favored and high selectivity to preferable products CH_3OH may be achieved.

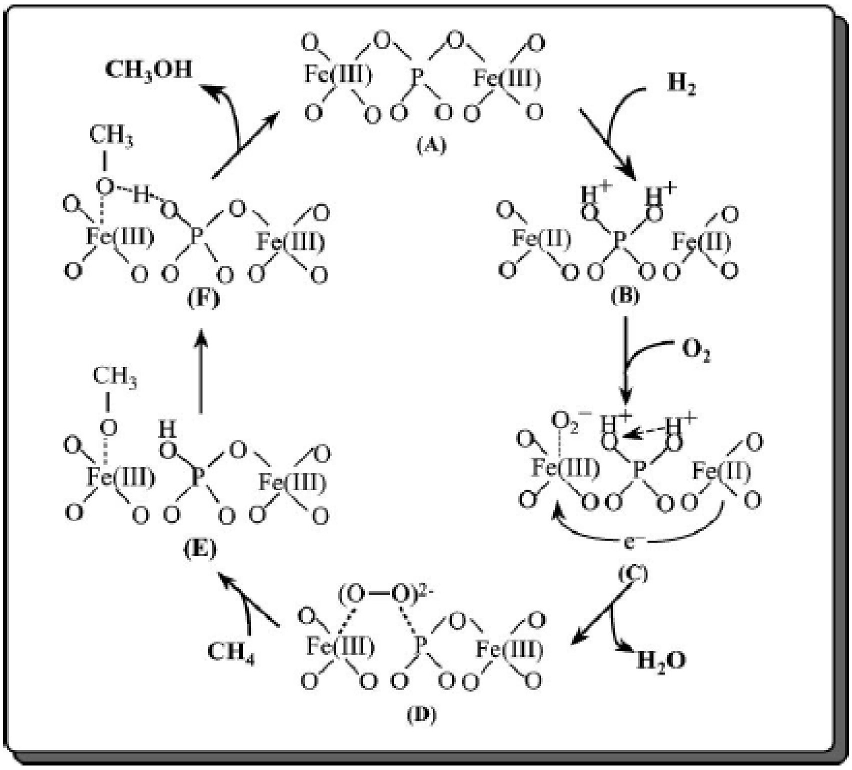

Fig. 2.7 Reaction mechanism for selective oxidation of CH_4 to CH_3OH by H_2-O_2 over $FePO_4$ catalyst with active iron sites [18].

For V_2O_5/SiO_2, charge transfer in surface lattice of vanadium oxide results active surface O species: $V^{5+} + O^{2-} = V^{4+} + O^{-}$. In formaldehyde formation, H_2 addition can decrease reaction temperature by 50 degrees. A moderate temperature reduce is required preserving CH_3OH. But low temperature will eliminate forming specific active center (from V^{4+} to V^{3+}) which decreases reaction rate sharply [19].

To avoid further oxidation of CH_3OH, transit reaction has also been considered. R. Burch published several articles focusing methane partial oxidation under transient reaction conditions. Unfortunately, main product is synthesis gas or formaldehyde.

$Fe_2(MoO_4)_3$ is the most active and selective catalyst among several molybdates for methane partial oxidation to formaldehyde under atmospheric pressure. Dope $Fe_2(MoO_4)_3$ with Zn, Li can enhance HCHO formation by inhibiting HCHO oxidation. If pure $Fe_2(MoO_4)_3$ doesn't work well, doping could be an option for improvement [31].

Iron-molybdate based catalysts are also used for side chain oxidation of alkylaromatics. Isolating iron molybdate active sites enhances selectivity to –CHO groups when activates $-CH_3$ groups. It gives higher selectivity compared to bulk iron molybdate in p-xylene(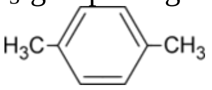) oxidation to para-tolualdehyde(PTA 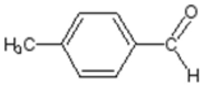) and terephthaloaldehyde(TPA 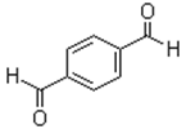) [32]. Active sites isolation may be a good option if a catalyst is too active, i.e. converts CH_4 to CO, CO_2 in methane oxidation. It provides a clue how to improve a catalyst performance which may be useful in my project.

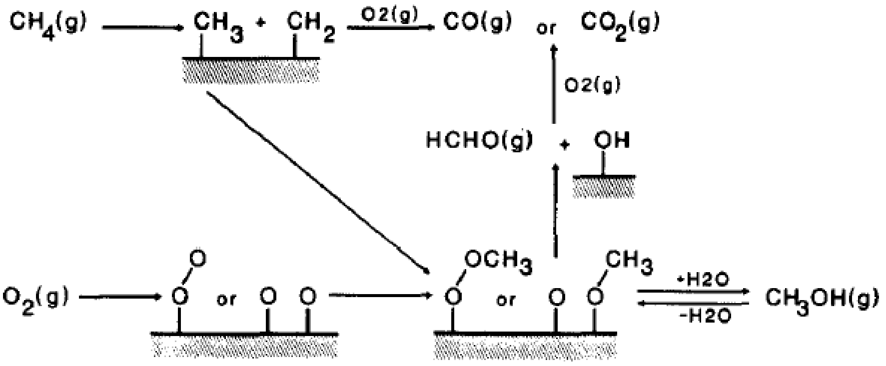

Fig.2.8 Surface scheme for the design of methane oxidation catalyst [30]

3 Experimental methods

3.1 Determination of total surface area

The physisorption of N_2 is utilized to measure the surface area of a solid material. The principle is physisorbed N_2 molecules form a monolayer covering the total area of the material at low temperature. The formed monolayer is independent of the atomic structure of the surface, only depends on the size of the molecule. Knowing the size of the molecule, one can then calculate the entire surface area. Multilayer will eventually form when enough gas is added.

The operation procedure is as follows. A sample is put into a glass chamber. To get rid of things (for example water) those are already adsorbed, the sample is dried under high temperature for several hours in a vacuum oven. This chamber is then installed on the BET equipment properly, cooled in a container filled with liquid nitrogen. After the machine evacuates the chamber and creates a vacuum, small portions of gaseous nitrogen is added to the chamber. After each injection, time is given for the system to reach equilibrium. Then a new injection is done, giving a new equilibrium, pressure etc. When a desired number of measurements have been done, the calculations based on the BET equation are done automatically by the computer connected to the machine and the specific surface area is obtained.

The experiment is performed at 77K and the measured parameter is pressure P. P_0, N_A/V_A should be given by standard data and the amount of added gas V is controlled by the instrument. V_m and C are calculated by the computer and are used to calculate surface area, SA.

The BET equation:

$$\frac{1}{V[(P_0/P)-1]} = \frac{C-1}{V_m}\left(\frac{P}{P_0}\right) + \frac{1}{V_m C}$$

P	Equilibrium pressure for a particular surface coverage
P_0	The saturated vapour pressure of the liquid adsorbate at the adsorption temperature
V	The volumetric uptake of gas at pressure P
C	constant

This is an equation in a linear form and a graph (Fig.3.1 b) is made. C and V_m are extracted from the slope and the intercept. Solving equation (1) and (2), the monolayer volume V_m will give the surface area (SA) in turn.

$$Slope = \frac{(C-1)}{V_m \cdot C} \qquad (1)$$

$$Intersect = \frac{1}{V_m \cdot C} \qquad (2)$$

$$SA = \frac{V_m \cdot N_A \cdot A}{V_A} \qquad (3)$$

N_A/V_A	Avogadro’s number per unit volume of gas
A	Area of the adsorbate molecule (0.16 nm^2 for N_2)

In order to get the specific surface area, SSA, the surface area is divided by the weight of the sample.

$$SSA = \frac{SA}{m}$$

m	Weight of the sample

Physisorption can be used to determine the distribution of pore volumes and pore sizes. The filling of pores with condensed adsorbate beyond a monolayer is related to the radius of the pores and the gas pressure. Smallest pores are most easily to be filled.

However, this idealized assumption doesn’t work in reality. Multilayer can form before completion of the monolayer and the BET equation is used since it better account for this phenomena. The BET equation actually applies to the region before monolayer are created, at low pressures when P/P_0 in the range between 0.05 – 0.30. But still a number of assumptions are made for the BET equation to work, e.g. the Langmuir theory can be applied, no adsorbate-adsorbate interaction.

The total surface area is important since a large support area could facilitate high surface area of the active component and hence good activity. But it should be stressed that N_2 adsorbs in a non-specific way and this method cannot be used to measure the active surface. When only look at the total surface area this won’t tell you how well dispersed the catalyst particles are.

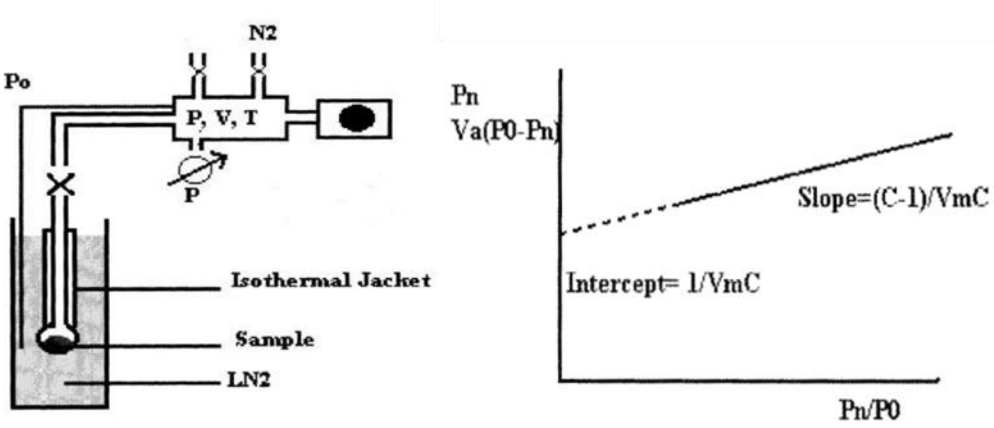

a **b**

Fig.3.1 a) Setup of BET and b) Graph using BET equation

3.2 X-ray diffraction for powder catalysts

Generation of X-rays:

An electrically heated filament, usually tungsten, emits electrons, which are accelerated by a high potential difference (20-50 kV) and allow striking a metal or anode which is water cooled (Fig.3.2). The anode emits a continuous spectrum of "white" X-radiation but superimposed on this are sharp, intense X-ray peaks (K_α K_β) as depicted. The frequency of the K_α and K_β lines are characteristic of the anode metal; the target metals most commonly used in X-ray crystallographic studies are copper and molybdenum, which have K_α lines at 154.18 pm and 71.07 pm respectively. These lines occur because the bombarding electrons knock out electrons from the innermost K shell (n=1) and this in turn creates vacancies which are filled by electrons descending from the shells above. The decrease in energy appears as radiation; electrons descending from the L shell (n=2) give the K_α lines and electrons from the M shell (n=3) give the K_β lines. As the atomic number, Z, of target atom increases, the lines shifts to shorter wavelength.

Normally in X-ray diffraction, monochromatic radiation is required. Usually the K_α line is selected and K_β line is filtered out by using a filter made of a thin metal foil of the element adjacent (Z-1) in the Periodic Table; thus nickel effectively filters out the K_β line of copper, and niobium is used for molybdenum. A monochromatic beam of X-rays can also be selected by reflecting the beam from a plane of a single crystal, normally graphite.

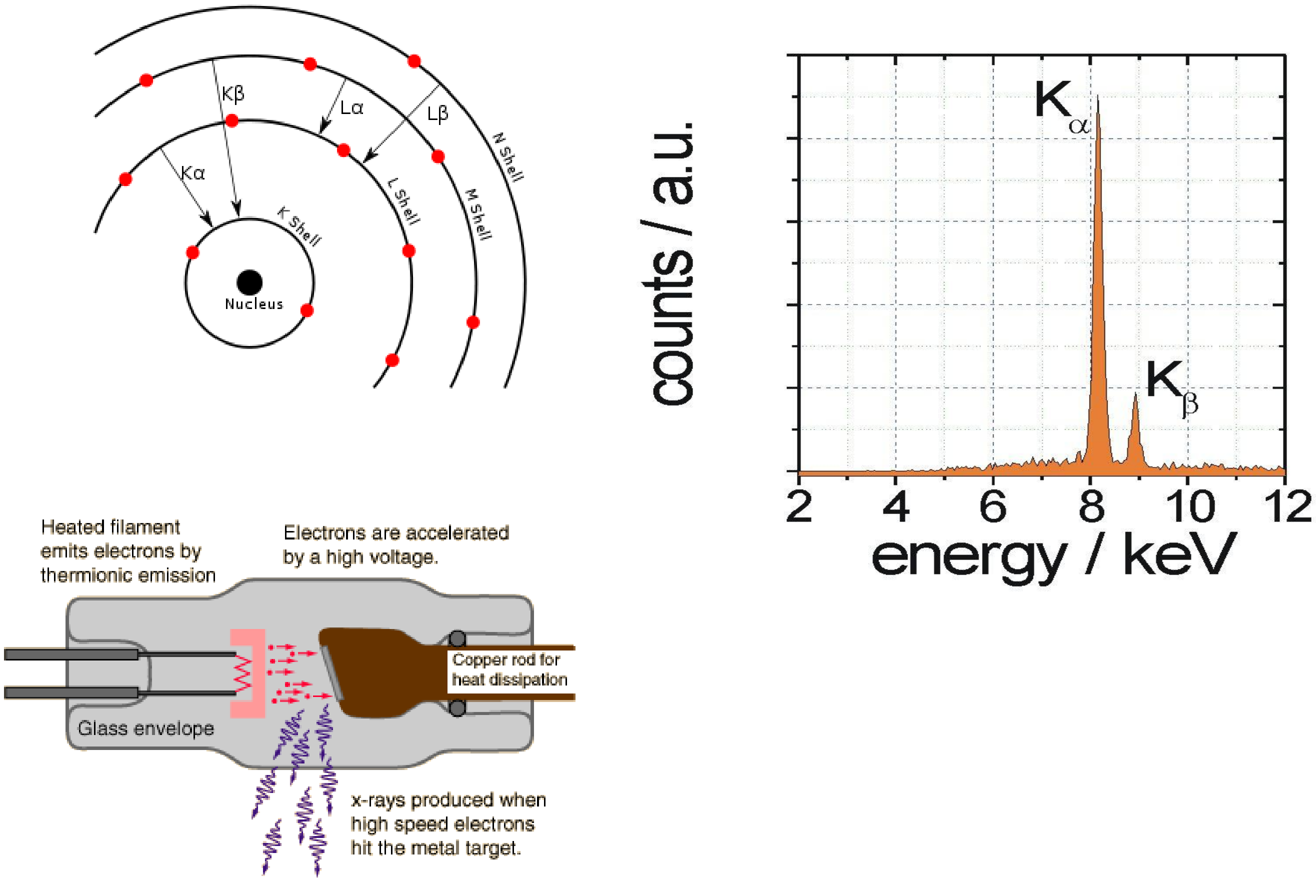

Fig.3.2 Working principle of X-ray diffraction experiment.

Diffraction of X-rays

Crystalline solids consist of regular arrays of atoms, ions or molecules with interatomic spacing of the order of 100 pm. For diffraction to take place, the wavelength of the incident light has to be the same order of magnitude as the spacing of the grating. Because of the periodic nature of the internal structure, it is possible for crystals to act as a three-dimensional diffraction grating to light of a suitable wavelength. X-ray diffraction behaves like 'reflected' from the planes of atoms within the crystal and that only at specific orientations of the crystal with respect to the source and detector are X-rays 'reflected' from the planes. It is not like reflection of light from a mirror, as this requires the angle of incidence equals the angle of reflection, and this is possible for all angles. With X-ray diffraction, the reflection only occurs when the constructive interference are fulfilled.

Bragg condition:

Bragg diffraction occurs when electromagnetic radiation or subatomic particle waves with wavelength comparable to atomic spacings, are incident upon a crystalline sample, scattered by the atoms in the system and undergo constructive interference in accordance to Bragg's law. For a crystalline solid, the waves are scattered from lattice planes separated by the interplanar distance d. If the scattered waves interfere constructively, they remain in phase since the path length of each wave is equal to an integer multiple of the wavelength. The path difference between two constructive interference waves is given by 2dsinθ, where θ is the scattering angle. This is Bragg's law, which describes the condition for constructive interference from successive crystallographic planes (h, k, l) of the crystalline lattice:

$$2d\sin\theta = n\lambda.$$

A diffraction pattern is obtained by measuring the intensity of scattered waves as a function of scattering angle. Very strong intensities known as Bragg peaks are obtained in the diffraction pattern where scattered waves satisfy the Bragg condition.

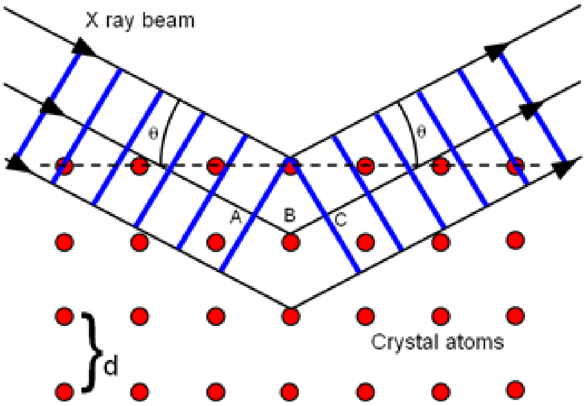

Fig.3.3 Diffraction of X-rays

Powder Diffraction

A finely ground crystalline powder contains a very large number of small crystals, known as crystallites, which are oriented randomly to one another. If such a sample is placed in the path of a monochromatic X-ray beam, diffraction will occur from planes in those crystallites which happen to be oriented at the correct angle to fulfill the Bragg condition. The sample was rotated and the incident X-ray beam was going up and down to bring as many planes as possible into the diffraction condition. A detector is used to record the angle and the intensity of the diffracted beams, which are plotted as intensity against 2θ. Thus the d (h, k, l) spacing for each reflection can be calculated.

3.3 Activity tests using continuous gas-flow reactor and mass spectrometry

Methane partial oxidation experiments were performed in a continuous gas-flow reactor in this project. Product stream was analyzed by a mass spectrometer connected with the reactor. A common set-up of a flow reactor is schematic presented in Fig. 3.4. Gases were introduced by mass flow controllers, which were controlled with a computer. The reactor tube was surrounded by metal coil for resistive heating and carefully insulated by quartz wool. Thermocouples were attached to measure temperature of the inlet gas. Due to that powder samples were investigated, a vertical tube as shown in Fig.3.5 was used for all experiments. The powder sample was put on a white porous quarts glass platform, which allows only the gas flow to pass through.

To monitor the composition of the outlet gas flow, a mass spectrometer (MS) was used. With a MS, both qualitative and quantitative measurements can be performed. The general principle used in mass spectrometry is that the sample gas (molecules) are separated by their mass-to-charge ratios by usage of a magnetic and/or electric fields. Uncharged molecules are ionized first. Mass analyzer separates the molecules/fragments and a detector is used to monitor the incoming ions.

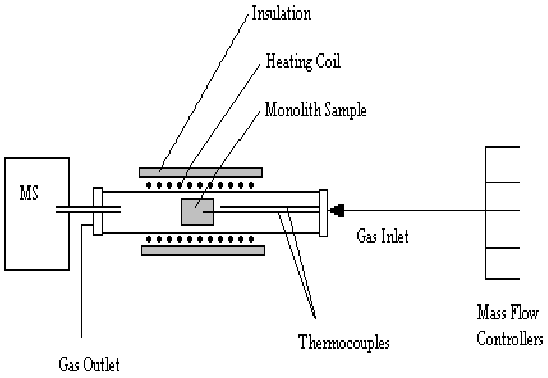

Fig.3.4 Horizontal flow reactor set-up

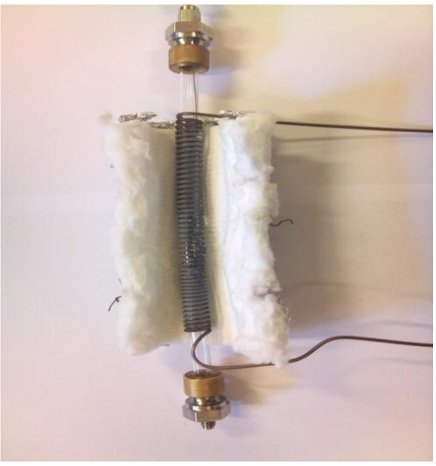

Fig.3.5 Vertical reactor tube together with heating coils and insulation

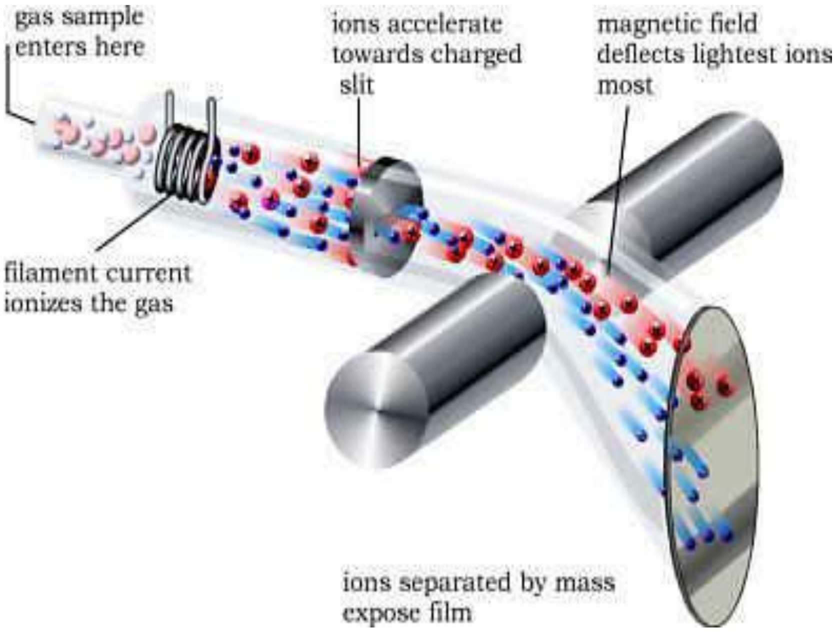

Fig.3.7 Schematic representation of mass spectroscopy principle [33]

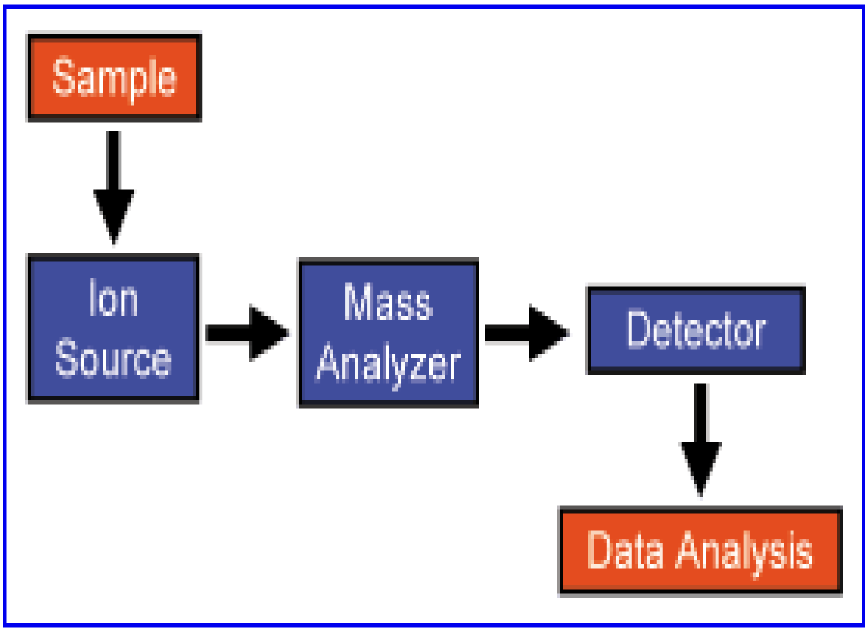

Fig.3.8 Main parts of a mass spectrometer

4 Experimental part

4.1 Catalyst preparation

In this project, two types of $Fe_2(MoO_4)_3$ were synthesized by hydrothermal treatment. Raw materials were analytic grade $Fe(NO_3)_3 \cdot 9H_2O$ (Sigma Aldric >98%) and $(NH_4)_6Mo_7O_{24} \cdot 7H_2O$ (Acros,>99%). 2* 88mL distilled water were added into 2.73g $Fe(NO_3)_3 \cdot 9H_2O$ and 1.79g $(NH_4)_6Mo_7O_{24} \cdot 7H_2O$ separately. After complete dissolution, the $(NH_4)_6Mo_7O_{24}$ solution was dropped into the $Fe(NO_3)_3$ solution under magnetic stirring to form a homogenous solution. The pH of the mixed solution was adjusted to pH=1.65 for sample no.1 and pH=3 for sample no.2 using $NH_3 \cdot H_2O$ (25 wt%) and HNO_3 (1 mol/L). Thereafter the precursor solution was transferred into a Teflon-lined autoclave and sealed. The autoclave was put into an oven for 12h at 140 ℃. Followed by hydrothermal treatment, the autoclave was cooled down to room temperature naturally. The synthesized $Fe_2(MoO_4)_3$ was then washed several times with distilled water and pure ethanol. Finally the samples were dried in a vacuum oven for 4h at 60 ℃ [34].

4.2 Flow reactor measurements

Flow reactor measurements

Methane partial oxidation experiments were performed in the gas-flow reactor mentioned above. The powder samples were positioned on a porous quartz plate permanently fixed inside the vertical tube. The inlet gas temperature was measured by a thermocouple (type k) about 10 mm above the sample bed. Gases were injected from the top of the tube and passed through the sample bed. A mass spectrometer was used to analyze product stream with respect to H_2 (m/e=2), CH_4 (m/e=15), CO (m/e=28), HCHO (m/e=29 and 30), CH_3OH (m/e=31), O_2 (m/e=32), CO_2 (m/e=44). In all cases, temperature was adjusted manually and kept constant before reactants injection. Gases employed were 2% CH_4/Ar, 2% O_2/Ar and 4% H_2/Ar. The total flow was 100 mL/min and the composition was composed by using individual mass flow controllers.

Partial oxidation of methane – pulse-response experiments

To study the impact of temperature and the effect of CH_4/O_2 ratio on the partial oxidation of methane over the two $Fe_2(MoO_4)_3$ samples, various experiments were carried out at different temperatures and different CH_4/O_2 ratio. The experiments were started by feeding x% O_2 for t=10min followed by addition of y% CH_4 also for 10 min at the temperature to be studied. The experiments then contained two parts for each temperature. First the O_2 concentration was kept constant while varying the CH_4 concentration, i.e. switch the CH_4 feed on (10 min) and off (10 min). Thereafter the CH_4 concentration was kept constant while the O_2 feed was switched on (10 min) and off (10 min). Table 4.2 shows a summary of all test conditions for the two samples.

Table 4.1.Experiment conditions of CH_4-O_2 group a. Temperature increased 50 degree every time

CH_4/O_2 ratio	CH_4 concentration	Experiment temperature
5:1	15000ppm	373K ~973K (a)
4:1	10000ppm	673K
		773K
		873K
		973K
3:1	9000ppm	673K
		773K
		873K
		973K

Influence of hydrogen on partial oxidation of methane

To study the effect of hydrogen addition on formation of products for the two samples, H_2 was introduced to the reactant gas stream. Similar as the CH_4/O_2 test described above, only one reactant was varied periodically while the remaining reactants were kept constant. The experiment contained three parts. First, the concentration of CH_4 and O_2 were kept constant while H_2 was switched on (10 min) and off (10 min). Thereafter, O_2 was switched on and off while CH_4 and H_2 were constantly fed. In the last part then, CH_4 was switched on and off keeping the O_2 and H_2 concentrations constant. In all other respects these experiments were following the same procedure as the experiments described above. For a summary of experimental conditions, see Table 4.2.

Table 4.2 Experiment conditions of CH_4-O_2-H_2 system

CH_4/O_2 ratio	CH_4 concentration	Experiment temperature	H_2 concentration
4:1	10000ppm	773K	500ppm
			1000ppm
		873K	500ppm
			1000ppm
		973K	500ppm
			1000ppm
3:1	9000ppm	773K	500ppm
			1000ppm
		873K	500ppm
			1000ppm
		973K	500ppm
			1000ppm

4.3 Characterization

To achieve structural information and characterize the total surface, XRD and N_2 physisorption measurements according to the BET method were carried out for fresh as well as heat and hydrogen treated samples. In the latter case, the samples were dried in a vacuum oven for 4h at 230 ℃ before surface area measurement.

The XRD experiments were carried out at the division Environmental inorganic chemistry (Professor Vratislav Langer).

5 Results and discussion

5.1 Synthesis

The pH value of precursor suspension has significant influence on crystallized $Fe_2(MoO_4)_3$ formation. The pH value 1.65 led to pale green product sample no.1 and pH 3 resulted brown product sample no.2.

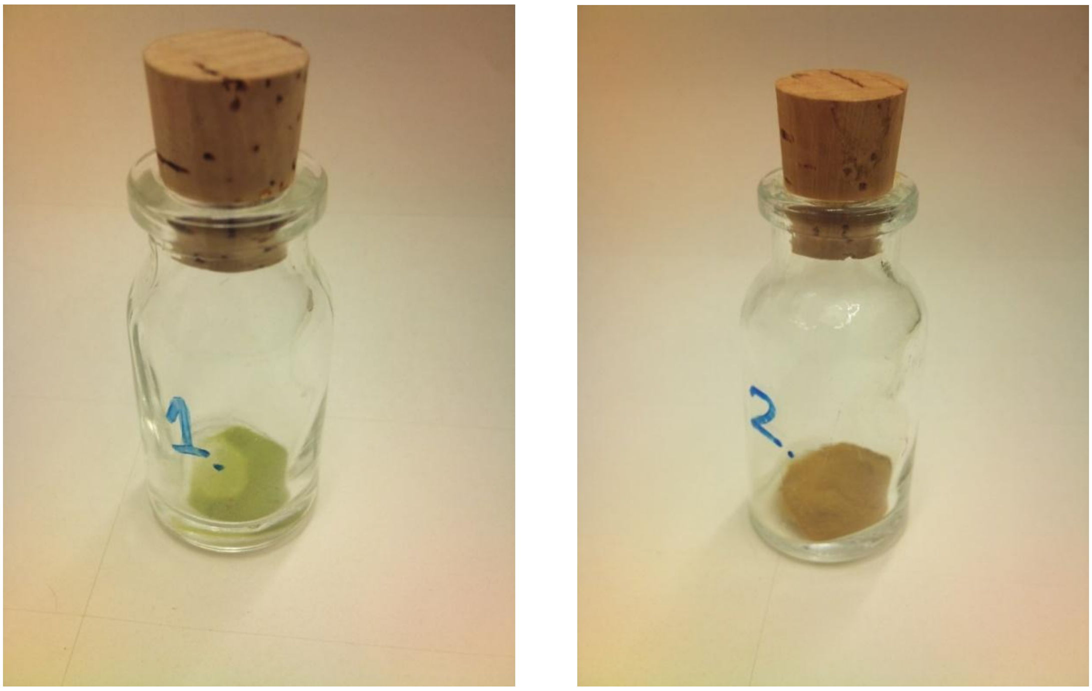

Fig.5.1 a *Fig.5.1 b*

a.sample no.1 synthesized from pH 1.65 solution b.sample no.2 synthesized from pH 3 solution

5.2 Partial oxidation of methane - pulse-response experiments

In this section the results from partial oxidation of methane are presented. Mainly, the influence of five different parameters are considered, i.e., i) reaction temperature, ii) catalyst preparation route, iii) CH_4/O_2 ratio iv) H_2 addition and v) the concentration of hydrogen.

Influence of reaction temperature

In Fig.5.2, the results from oxidation of 10000 ppm CH_4 using 2500 ppm O_2 over 0.4177g sample no.2 during reactant pulsing described above at three different temperatures, i.e., 673K (blue), 873K (green) and 963K (red) are shown. The top panel displays the reactants changes during the test. The remaining panel then show the the signals for the products HCHO, CO and CO_2. Due to the cracking pattern in the ionization of the product gas HCHO contributes to both m/z 29 and 30.

At t=10min, 2500ppm O_2 is introduced. It can be seen as a rapid increase of O_2 in outlet gases at 673K, for 873K and 963K the increase in O_2 concentration is somewhat slower. This reflects higher adsorption of oxygen at higher temperature which may imply that the O_2 adsorption process is activated. After a short period, about 2min for 673K and about 5-6min for 873K and 963K case, the O_2 concentration stabilizes at a certain level. At t=20min, 10000 ppm CH_4 is injected into the reactor tube. Similar as for the introduction of O_2, the fastest increasing response, although now for CH_4, is observed for the lowest temperature followed by the other temperatures. At 673K, CH_4 signal reaches steady condition shortly after the injection. For the other cases, CH_4 reaches maximum only at the end of CH_4 on pulse close to t=30min. As can be seen, the CH_4 peak concentrations reach different levels. The higher the reaction temperature, the lower CH_4 concentration in the outlet gases indicates a higher reaction rate for methane oxidation at higher temperature, at least transiently. Immediately after injection of CH_4 the products HCHO, CO and CO_2 can be observed. The concentration of products keeps increasing and reaches maximum concentration at the highest CH_4 concentration. This can be read in different panels as product signals start increasing at t=10min and arrive tops at t=30min. Products share the same trends with CH_4. Before CH_4 injection, the catalyst surface is likely already covered with activated oxygen species. When CH_4 is switched on, it reacts with surface O_2 species immediately with a simultaneous formation of products. In first step, CH_4 goes through lean and rich conditions. But it seems that no productivity appears. Otherwise, straight line segment can be seen in product signals. The variation of O_2 signal during CH_4 on-off process is difficult to explain but may, unfortunately, be due to changes in the total flow during pulsing. By comparing the differences between 873 to 673K and 963 to 673K the amount of consumed O_2 can be estimated. Obviously, more O_2 is consumed when the temperature is increased. During CH_4 off periods, CH_4 decreases slower at 963K compared with 873K and 673K. Furthermore, it reaches higher levels than for 873K and 673K. This could be due to the release of surface adsorbed CH_4 molecules or recombination of CH_x and hydrogen species to form methane. Analogous to the CH_4 switch-off, the O_2 response during O_2 switch off at t=80 min decreases slower at the higher temperatures which could be due to desorption of O_2.

At t=90min, the second part of the experiment starts. At first only methane is injected to the reactor. All product signals increase immediately when CH_4 is introduced. Rapid response of product signals may be due to the reaction between remaining active surface oxygen species. The increasing trend of the CH_4 signal is similar as for the CH_4 on/off cycling above. At t=100min the CH_4 signal is stable. The pulsing of oxygen starts at t=100 min. During O_2 on and off process, product signals vary. The product signal peaks correspond to the O_2 signal peaks. Easily can be seen, during O_2 off periods, O_2 decreases slower at 963K and reaches higher levels than for 873K and 673K. This may indicate a O_2 supply by catalyst. The release of oxygen from bulk or recombination of activated oxygen species to form oxygen may be the sources.

In summary, the higher the reaction temperature the higher CH_4 and O_2 consumptions and product concentrations. Also, the oxygen release from catalysts is higher.

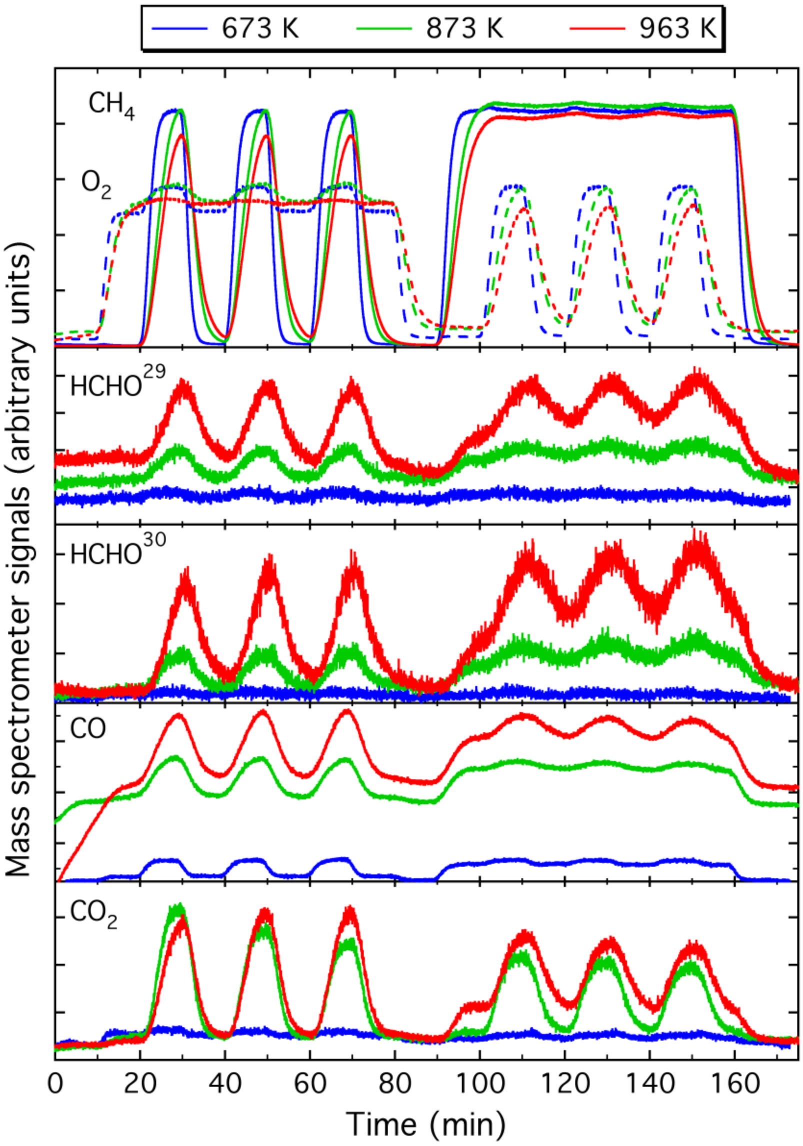

Fig.5.2 Temperature influence. CH_4 conc. 10000ppm, $CH_4/O_2=4$, over 0.4177g sample no.2

Influence of sample preparation route

Fig.5.3 displays data over the different samples at 873K using 10000ppm CH_4 and 2500ppm O_2. Black curve are results obtained over 0.4177g no.1 sample and red curve shows results obtained over 0.5713g no.2 sample.

Although most parts of Fig.5.3 are almost the same as description for Fig.5.2, some differences will be pointed out. At time range t=100 to 160 min, the CH_4 signals for the two samples are close although the product signals for sample number two is significantly higher than for sample one. The reason for the "missing methane" may be methanol production over sample one. Unfortunately, methanol is not able to be measured in this project. Under the present reaction conditions, the product signals are usually lower for sample no.1 as compared to sample no.2. This indicates that sample no.1 is less active in forming HCHO, CO and CO_2 than sample no.2 during experimental conditions, but may be more active in methanol production.

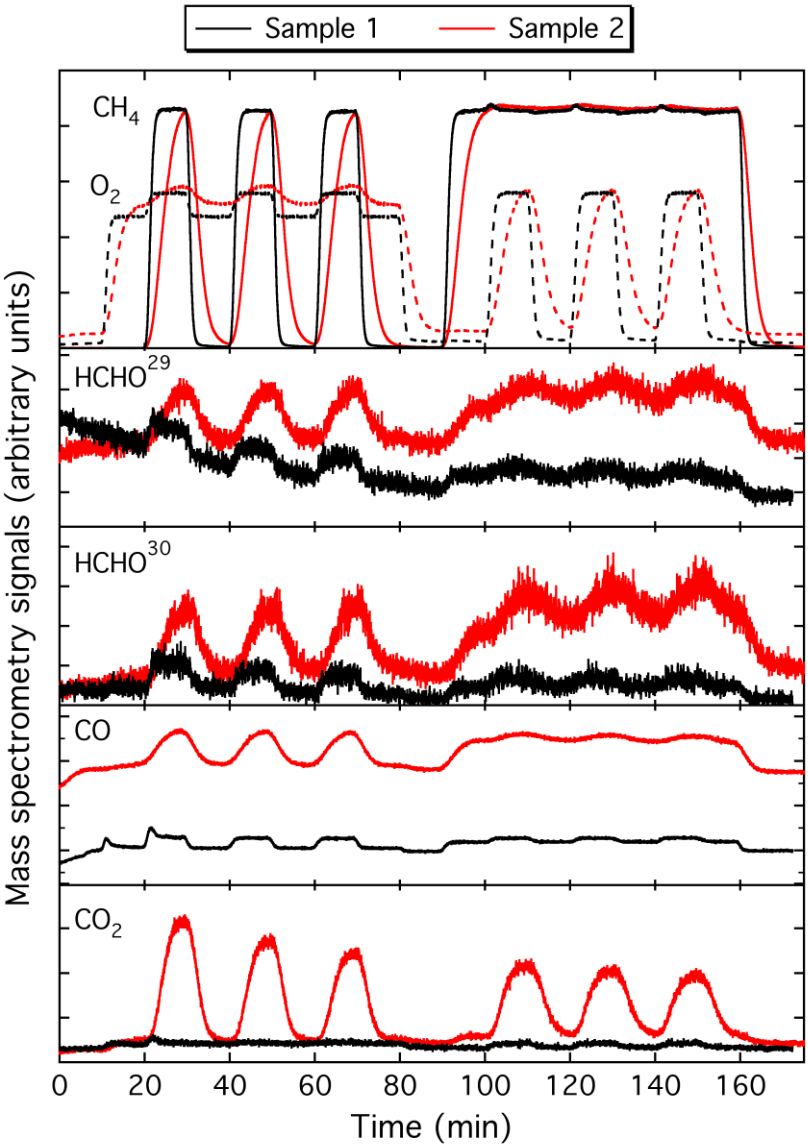

Fig.5.3 Catalyst impact. CH_4 conc.10000ppm, CH_4/O_2=4, T=873K. 0.4177g sample no.1 and 0.5713g sample no.2

Influence of CH_4/O_2 ratio

As shown in Table.4.1, tests were performed for different concentrations of CH_4 and O_2, i.e., CH_4/O_2 ratio of 5,4 and 3. For $CH_4/O_2=5$, no changes in product signals were found as compared to $CH_4/O_2=4$ as shown in Fig.5.3, thus in Fig.5.4 data for $CH_4/O_2=3$ and 4 is shown. For $CH_4/O_2=3$, CH_4 concentration is 9000 ppm, O_2 concentration is 3000 ppm and for $CH_4/O_2=4$, CH_4 concentration is 10000 ppm, O_2 concentration is 2500 ppm.

As can be seen in the top panel, the CH_4 signals and O_2 signals for the two gas ratios are very similar during the methane on-off cycling (the CH_4 signal may be sligtly higher in general). The same is obsrved for the HCHO product. However, turning to the other product panels, the CO and CO_2 signals are apparently higher in the case of $CH_4/O_2=4$. It seems that instead of inhibiting complete oxidation, higher CH_4 concentration promotes methane oxidation further to CO and CO_2 (more favored to CO_2) over the tested samples. Or in other words, lower oxygen concentration results in higher CO and CO_2 production. This may indicate that the partial oxidation of methane is sensitive to oxygen concentration, i.e., the catalyst may suffer from oxygen poisoning. Even more interesting is that since the CH_4 consumption is similar in the two cases, the lower ratio may lead to formation of products not measured in the present experiment, i.e., methanol.

The difference in CO signals between, on the one hand, CH_4 on/off cycling and, on the other hand, O_2 on/off cycling is most likely due to that in the first case, it is the reactant containing the carbon that is shut on and off leading to more clear peaks in the CO (and CO_2 signals). Interestingly, when performing O_2 on/off cycles, it is the CO_2 that varies most. This supports further that selectivity is strongly connected to the CH_4/O_2 ratio as this ratio changes in the transient during pulsing.

To summarize, CH_4/O_2 ratio has strong influence on product selectivity. Higher methane concentration promotes further oxidation products CO and CO_2.

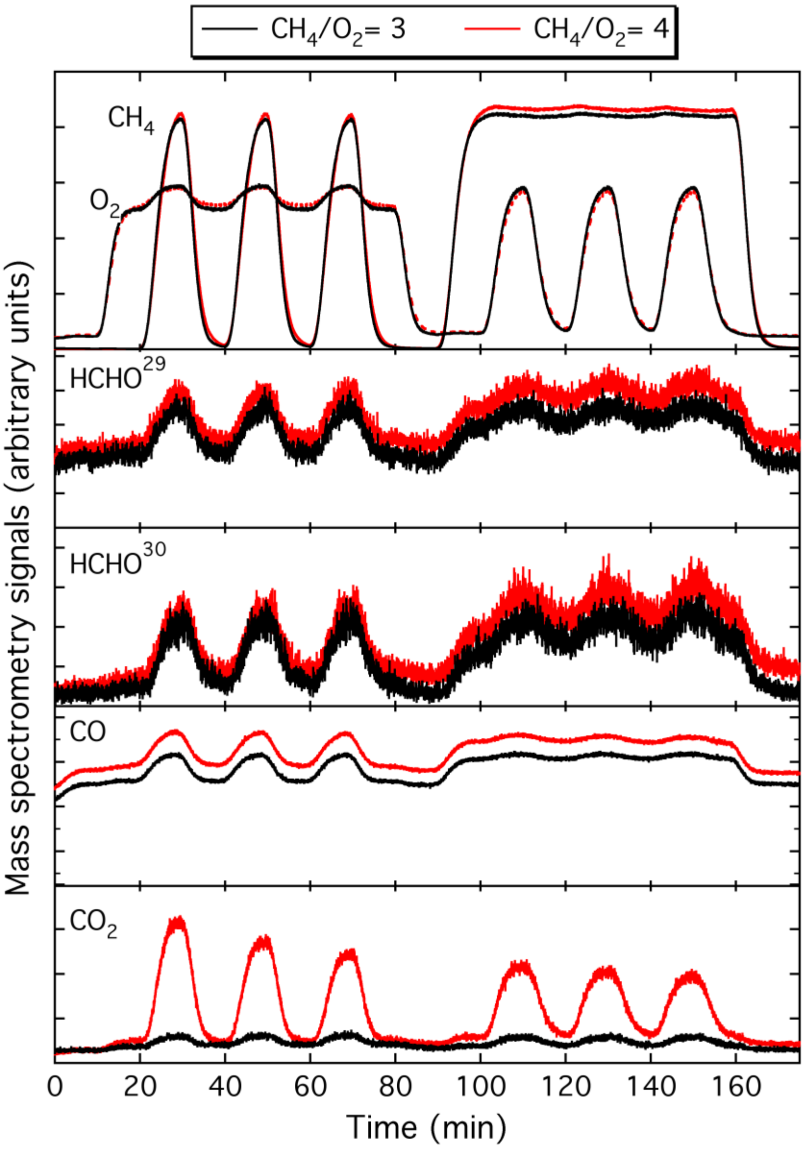

Fig.5.4 The effect of different CH_4/O_2 ratio. For $CH_4/O_2=4$, $CH_4=10000ppm$, $O_2=2500ppm$. For $CH_4/O_2=3$, $CH_4=9000ppm$, $O_2=3000ppm$. Experiments were performed at 873K over 0.5713g sample no.2

Influence of hydrogen addition

In this and next section the results obtained when a small amount H_2 is introduced to the reactant stream will be discribed. The focus is on the most important differences between the experiments. Each test contains three parts. In the first part, CH_4 and O_2 were kept constant while H_2 was switched on and off. In the second part, O_2 was switched on and off while CH_4 and H_2 were supplied at constant level. In the last part then the O_2 and H_2 were kept constant while CH_4 was switched on and off.

Fig.5.5 shows the experiment with T=873K, 9000 ppm CH_4, 3000 ppm O_2 and 1000 ppm H_2. The amount of catalyst was 0.5713g for sample no.1 and 0.5653g for sample no.2.

In the top panel it can be seen that O_2 signals start to decrease/increase when H_2 is switch on/off. The highest H_2 signals correspond to the lowest O_2 signals and vice versa. In the product panels, all signals follow almost straight lines, no fluctuation appear. Signals obtained over sample no.1 are slightly higher than those obtained over sample no.2. In the second part, the relationship between O_2 and H_2 is the same as for the first part. Despite this, the CH_4 signal over no.1 sample shows obvious fluctuations. The signals over no.1 sample during period t=90 -170 min will be commented in more detail here.

At t=90min, CH_4 and H_2 are injected into the reactor. After 10 min both of them reach the highest level. When O_2 is switched on the H_2 signal drops immediately and vice versa. For sample 1, the CH_4 signal is not stable even though constant CH_4 is supplied. It follows the change trend of O_2 signals. It is clear that the variation of the CH_4 and O_2 signals are in counterphase with the variations in the H_2 signal. In general the product signals are higher for sample 1. For HCHO (m/e=29 signal) the variation is in phase with the corrsponding variations in the H_2 signal for both samples. This could be due to that O_2 and H_2 react to form water and thereby creating vaccant sites that may serve for partial oxidation of methane into HCHO. A more close look at CO and CO_2 signals reveals that during O_2 on/off cycling double peaks are observed. The first peak is smaller than the second. This phenomenon is more apparent for the CO_2 signal. The respective first maximum appears at t=100, 120, 140 and 160 min. At those times, the H_2 signals are in peak positions, while both CH_4 and O_2 signals are at minimum. The second maximum appears at 105, 125 and 145 min respectively. At these times the CH_4 and O_2 signals are increasing and H_2 signal is decreasing. The CO_2 shows minimum at times 115, 135 and 155 min. Contrary to the second maximum condition, CH_4 and O_2 are decreasing and the H_2 is increasing. The hydrogen signals in the first part of the experiment is generally lower than in the second part. This can be due to that in the first part of the experiment, the O_2 is constantly supplied and thus hydrogen reaction may occur each time H_2 is injected. In contrast, the second part of the experiment, O_2 is shut on and off which means that the outlet hydrogen signal can reach higher levels in the oxygen free periods. The double peaks may be due to that the surface composition changes between reactant deficiency conditions and reactant poisoning conditions. In the last part, all product signals follow the variations in CH_4 signal except the CO_2 signal. The maximum of CO_2 signal appears when the CH_4 signal reaches its lowest level. This may be due to that under these conditions, the catalyst surface is mainly occupied by active O_2 species so that incoming CH_4 molecules sense lean conditions. In this case, minor part of the CH_4 molecules can be adsorbed on the catalyst surface. The CH_4 species that are adsorbed react then to form CO_2 as the main product.

As a summary, additive H_2 enhances product formation may due to react with O_2 and influences more serious on sample no.1.

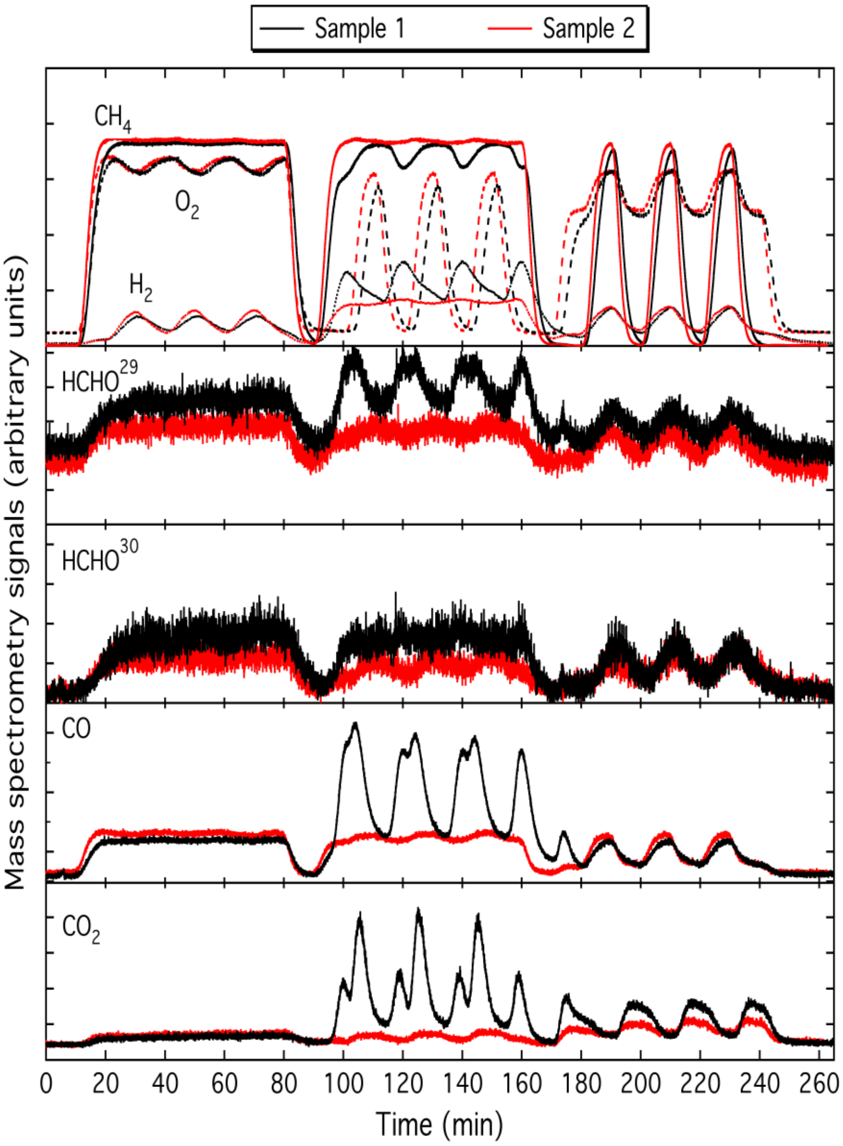

Fig. 5.5 Additive H_2 effect on the methane partial oxidation over different catalysts. Experimental conditions: $CH_4/O_2=3$ $CH_4=9000ppm$, $H_2=1000ppm$,$T=873K$ Weight of catalysts: sample no.1=0.5713g sample no.2= 0.5653g

Influence of hydrogen concentration

The effect of H_2 concentration for sample no.1 is shown in Fig.5.6. An increase of the hydrogen concentration results in higher CH_4 signal and lower HCHO, CO and CO_2 signals while the CO_2 signal on the first and third step which is somewhat higher. This may due that more oxygen is consumed by H_2 forming H_2O, in turn less O_2 contributes to methane oxidation reaction. Another trend, is that high H_2 conentration produces more obvious double peaks in the CO_2 signal.

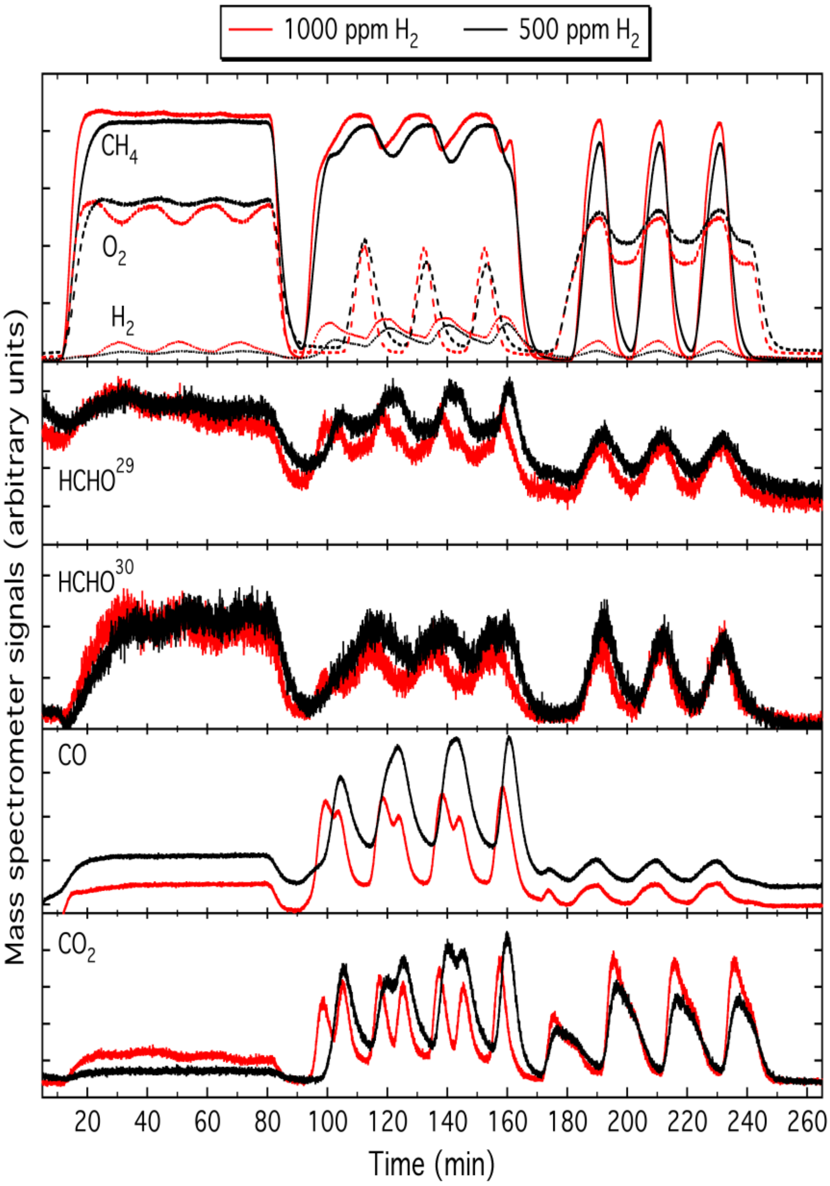

Fig.5.6 H_2 concentration effect on the methane partial oxidation over 0.5713g sample no.1. Experiments carried out at 935K with CH_4 conc. 1000ppm, CH_4/O_2=4.

5.3 Characterization of catalyst samples

5.3.1 Surface area

Surface area of fresh catalysts, catalysts after heat and H_2 treatment were measured. Results are given by Table 5.1.

Fresh sample has larger BET surface area compared with samples after treatments. While between fresh samples, the surface area of sample no.2 is more than four times larger than sample no.1. This could be one reason that sample no.2 is more active as discussed in *influence of sample preparation route* part. Surface area decreasing may due to sintering of sample particles during experiments.

Table 5.1 BET surface area for the catalysts after different treatments

	Fresh	After heat treatment	After H_2 treatment
Sample no.1	3.9315 m^2/g	0.8777 m^2/g	0.2364 m^2/g
Sample no.2	16.2980 m^2/g	0.2110 m^2/g	0.2230 m^2/g

5.3.2 XRD results

In Fig. 5.7—5.9, the XRD patterns for the two samples are shown. In Fig. 5.7, no significant difference is observed except for the single peak at $2\theta \approx 13°$. The monoclinic form of $Fe_2(MoO_4)_3$ is the only structure indicated in sample no. 2 at room temperature. While monoclinic $MoO_{2.4}(OH)_{0.6}$ responses several peaks in sample no.1 XRD pattern. Even though, for sample no.1 the main crystalline structure is still monoclinic $Fe_2(MoO_4)_3$. This contradicts to an article which acclaimed that the color difference of the samples results from crystalline structure. It says pale green sample is monoclinic $Fe_2(MoO_4)_3$ while the brown one is orthorhombic $Fe_2(MoO_4)_3$. Based on information given by database, orthorhombic $Fe_2(MoO_4)_3$ is stable above 772K (see Table 5.2). In another word, orthorhombic $Fe_2(MoO_4)_3$ should not appear at room temperature. Dissimilar Fe oxidation states in either sample may be the reason inducing distinct colors.

Fig.5.8 shows XRD patterns of fresh and treated sample no.1. As can be seen, XRD pattern shifts after treatments compared with fresh. H_2 treatment pattern shifts more obvious than heat treated one. Comparing with information provided by database, it suggests that monoclinic $MoO_{2.4}(OH)_{0.6}$, monoclinic $Fe_2(MoO_4)_3$ and orthorhombic $Fe_2(MoO_4)_3 \cdot 6.3H_2O$ all exit in heat treated sample. While in hydrogen treated sample, monoclinic $Fe_2(MoO_4)_3$, monoclinic $H_{1.67}MoO_3$ and also hexagonal FeO(OH) pattern can be found. In Fig.5.9, no crucial shift is observed for sample no.2. All fresh and treated sample apply the monoclinic $Fe_2(MoO_4)_3$ structure. The structural complexity of no.1 sample may be a factor for its distinct behavior in methane partial oxidation.

Table 5.2 Orthorhombic $Fe_2(MoO_4)_3$ information from database

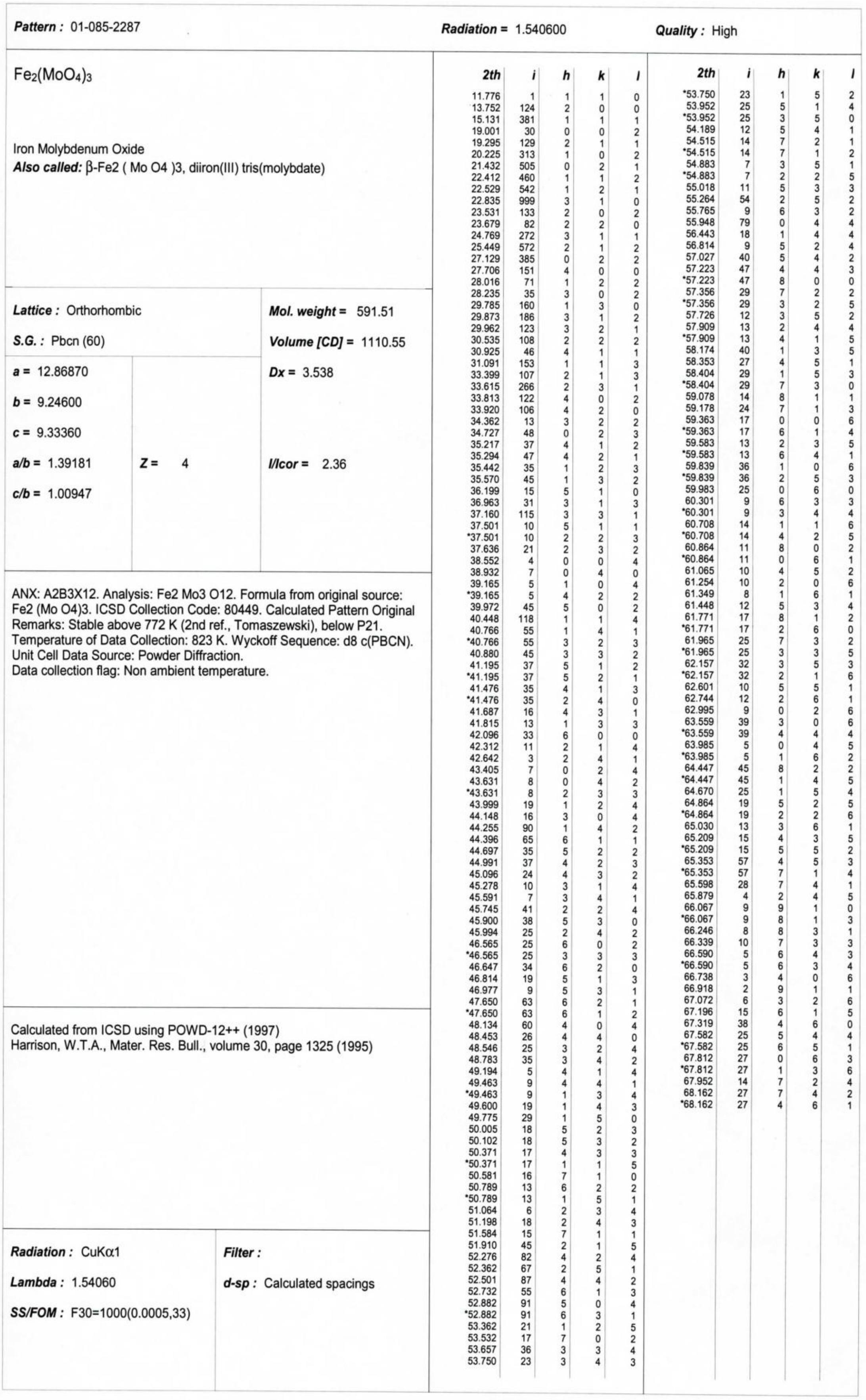

Pattern : 01-085-2287

Radiation = 1.540600

Quality : High

$Fe_2(MoO_4)_3$

Iron Molybdenum Oxide
Also called: β-Fe2 (Mo O4)3, diiron(III) tris(molybdate)

Lattice : Orthorhombic

S.G. : Pbcn (60)

a = 12.86870

b = 9.24600

c = 9.33360

a/b = 1.39181

c/b = 1.00947

Z = 4

Mol. weight = 591.51

Volume [CD] = 1110.55

Dx = 3.538

I/Icor = 2.36

ANX: A2B3X12. Analysis: Fe2 Mo3 O12. Formula from original source: Fe2 (Mo O4)3. ICSD Collection Code: 80449. Calculated Pattern Original Remarks: Stable above 772 K (2nd ref., Tomaszewski), below P21. Temperature of Data Collection: 823 K. Wyckoff Sequence: d8 c(PBCN). Unit Cell Data Source: Powder Diffraction.
Data collection flag: Non ambient temperature.

Calculated from ICSD using POWD-12++ (1997)
Harrison, W.T.A., Mater. Res. Bull., volume 30, page 1325 (1995)

Radiation : CuKα1

Lambda : 1.54060

SS/FOM : F30=1000(0.0005,33)

Filter :

d-sp : Calculated spacings

2th	i	h	k	l
11.776	1	1	1	0
13.752	124	2	0	0
15.131	381	1	1	1
19.001	30	0	0	2
19.295	129	2	1	1
20.225	313	1	0	2
21.432	505	0	2	1
22.412	460	1	1	2
22.529	542	1	2	1
22.835	999	3	1	0
23.531	133	2	0	2
23.679	82	2	2	0
24.769	272	3	1	1
25.449	572	2	1	2
27.129	385	0	2	2
27.706	151	4	0	0
28.016	71	1	2	2
28.235	35	3	0	2
29.785	160	1	3	0
29.873	186	3	1	2
29.962	123	3	2	1
30.535	108	2	2	2
30.925	46	4	1	1
31.091	153	1	1	3
33.399	107	2	1	3
33.615	266	2	3	1
33.813	122	4	0	2
33.920	106	4	2	0
34.362	13	3	2	2
34.727	48	0	2	3
35.217	37	4	1	2
35.294	47	4	2	1
35.442	35	1	2	3
35.570	45	1	3	2
36.199	15	5	1	0
36.963	31	3	1	3
37.160	115	3	3	1
37.501	10	5	1	1
*37.501	10	2	2	3
37.636	21	2	3	2
38.552	4	0	0	4
38.932	7	0	4	0
39.165	5	1	0	4
*39.165	5	4	2	2
39.972	45	5	0	2
40.448	118	1	1	4
40.766	55	1	4	1
*40.766	55	3	2	3
40.880	45	3	3	2
41.195	37	5	1	2
*41.195	37	5	2	1
41.476	35	4	1	3
*41.476	35	2	4	0
41.687	16	4	3	1
41.815	13	1	3	3
42.096	33	6	0	0
42.312	11	2	1	4
42.642	3	2	4	1
43.405	7	0	2	4
43.631	8	0	4	2
*43.631	8	2	3	3
43.999	19	1	2	4
44.148	16	3	0	4
44.255	90	1	4	2
44.396	65	6	1	1
44.697	35	5	2	2
44.991	37	4	2	3
45.096	24	4	3	2
45.278	10	3	1	4
45.591	7	3	4	1
45.745	41	2	2	4
45.900	38	5	3	0
45.994	25	2	4	2
46.565	25	6	0	2
*46.565	25	3	3	3
46.647	34	6	2	0
46.814	19	5	1	3
46.977	9	5	3	1
47.650	63	6	2	1
*47.650	63	6	1	2
48.134	60	4	0	4
48.453	26	4	4	0
48.546	25	3	2	4
48.783	35	3	4	2
49.194	5	4	1	4
49.463	9	4	4	1
*49.463	9	1	3	4
49.600	19	1	4	3
49.775	29	1	5	0
50.005	18	5	2	3
50.102	18	5	3	2
50.371	17	4	3	3
*50.371	17	1	1	5
50.581	16	7	1	0
50.789	13	6	2	2
*50.789	13	1	5	1
51.064	6	2	3	4
51.198	18	2	4	3
51.584	15	7	1	1
51.910	45	2	1	5
52.276	82	4	2	4
52.362	67	2	5	1
52.501	87	4	4	2
52.732	55	6	1	3
52.882	91	5	0	4
*52.882	91	6	3	1
53.362	21	1	2	5
53.532	17	7	0	2
53.657	36	3	3	4
53.750	23	3	4	3
*53.750	23	1	5	2
53.952	25	5	1	4
*53.952	25	3	5	0
54.189	12	5	4	1
54.515	14	7	2	1
*54.515	14	7	1	2
54.883	7	3	5	1
*54.883	7	2	2	5
55.018	11	5	3	3
55.264	54	2	5	2
55.765	9	6	3	2
55.948	79	0	4	4
56.443	18	1	4	4
56.814	9	5	2	4
57.027	40	5	4	2
57.223	47	4	4	3
*57.223	47	8	0	0
57.356	29	7	2	2
*57.356	29	3	2	5
57.726	12	3	5	2
57.909	13	2	4	4
*57.909	13	4	1	5
58.174	40	1	3	5
58.353	27	4	5	1
58.404	29	1	5	3
*58.404	29	7	3	0
59.078	14	8	1	1
59.178	24	7	1	3
59.363	17	0	0	6
*59.363	17	6	1	4
59.583	13	2	3	5
*59.583	13	6	4	1
59.839	36	1	0	6
*59.839	36	2	5	3
59.983	25	0	6	0
60.301	9	6	3	3
*60.301	9	3	4	4
60.708	14	1	1	6
*60.708	14	4	2	5
60.864	11	8	0	2
*60.864	11	0	6	1
61.065	10	4	5	2
61.254	10	2	0	6
61.349	8	1	6	1
61.448	12	5	3	4
61.771	17	8	1	2
*61.771	17	2	6	0
61.965	25	7	3	2
*61.965	25	3	3	5
62.157	32	3	5	3
*62.157	32	2	1	6
62.601	10	5	5	1
62.744	12	2	6	1
62.995	9	0	2	6
63.559	39	3	0	6
*63.559	39	4	4	4
63.985	5	0	4	5
*63.985	5	1	6	2
64.447	45	8	2	2
*64.447	45	1	4	5
64.670	25	1	5	4
64.864	19	5	2	5
*64.864	19	2	2	6
65.030	13	3	6	1
65.209	15	4	3	5
*65.209	15	5	5	2
65.353	57	4	5	3
*65.353	57	7	1	4
65.598	28	7	4	1
65.879	4	2	4	5
66.067	9	9	1	0
*66.067	9	8	1	3
66.246	8	8	3	1
66.339	10	7	3	3
66.590	5	6	4	3
*66.590	5	6	3	4
66.738	3	4	0	6
66.918	2	9	1	1
67.072	6	3	2	6
67.196	15	6	1	5
67.319	38	4	6	0
67.582	25	5	4	4
*67.582	25	6	5	1
67.812	27	0	6	3
*67.812	27	1	3	6
67.952	14	7	2	4
68.162	27	7	4	2
*68.162	27	4	6	1

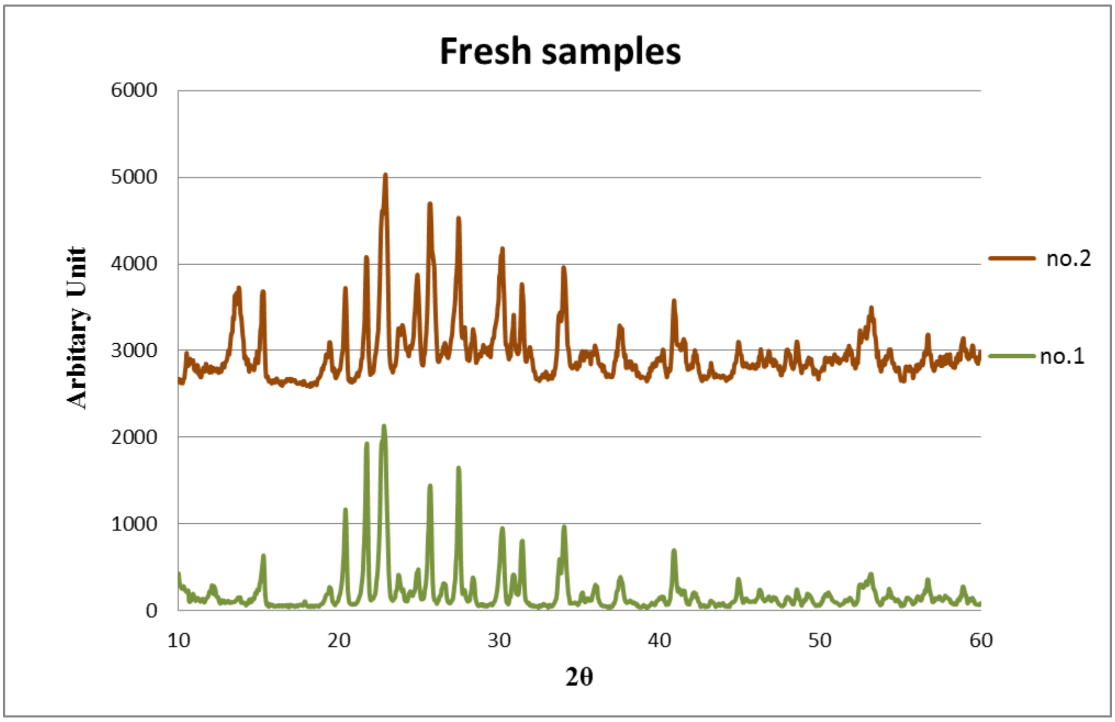

Fig. 5.7 XRD patterns of fresh samples

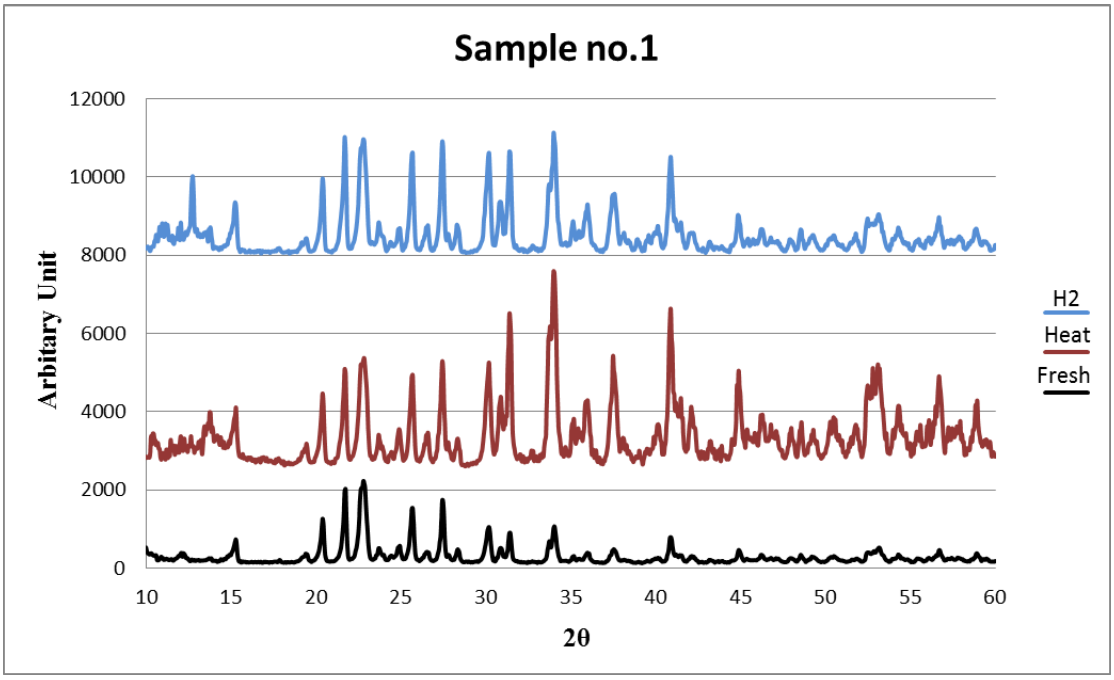

Fig.5.8 XRD patterns of sample no.1 before and after treatments

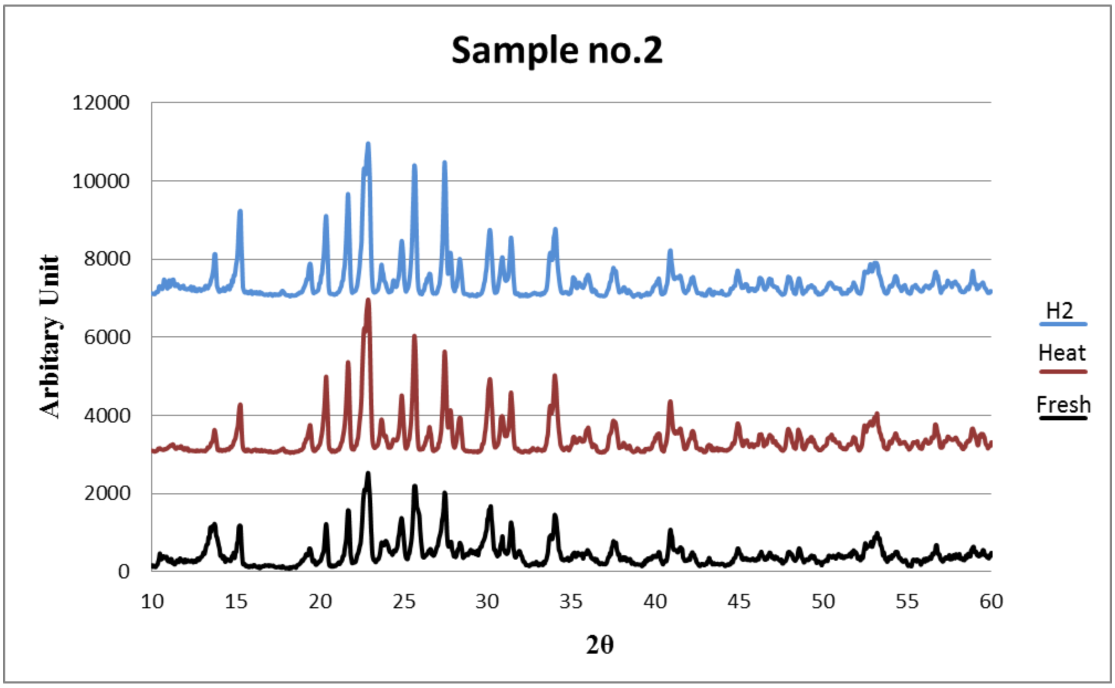

Fig.5.9 XRD patterns of sample no.2 before and after treatments

6 Concluding remarks

Experimental results for partial oxidation of methane over hydrothermally prepared $Fe_2(MoO_4)_3$ catalysts have been presented. In particular, the influence of i) reaction temperature, ii) catalyst preparation route, iii) CH_4/O_2 ratio iv) H_2 addition and v) the concentration of hydrogen on the CH_4 conversion have been investigated. Pulse-response experiments reveal that the reaction is promoted by high temperature and also is very sensitive to reactant composition. Addition of H_2 shifts the product selectivity to some extends. Both samples seem to store/release oxygen in during rich/lean cycling. The results indicate that methanol may be produced in small amounts for certain reaction conditions.

7 Future work

It would be interesting to use *in situ* DRIFT or other spectroscopic methods in combination with MS as to correlate surface species with reaction products during transient experimental conditions.

The variation of CH_4/O_2 ratio can be extended for further investigations on activity/selectivity.

It is also interesting to study gas additives like N_2O to influence the activity and selectivity and to get insights to (indications on) underlying mechanisms.

Mechanistic studies and theoretical modeling of reaction kinetics can be carried out in order to improve the fundamental understanding of the catalytic cycle.

8 Acknowledgement

I would like to express my sincere gratitude to my examiner, Professor Magnus Skoglundh, for giving me the opportunity working in such an interesting project and the support along the way.

I am very grateful to my supervisor, Per-Anders Carlsson, for all guidance, help and support from the first day of the project. All the discussions and talks benefit me a lot. Thanks for your suggestions during the project. They make me know how to work as a real researcher. Working together with you is such a great experience, I will never forget that.

I would like to give a special thank you to Professor Vratislav Langer, for running XRD tests and interpreting the results for me.

I am also deeply thankful to all the members in KCK group, Lisa Kylhammar and Elin Becker for making the reactor work properly; Fredrik Gunnarsson for finding things I needed when synthesizing; Malin Berggrund for those valuable discussions when I processed data; Hannes Kannisto for nice talking, tips when I hunting Ph.D. positions, strategy for innebandy and also recipe for “golden mushroom”.

Furthermore, I would like to express gratitude to all the people working in Applied Surface Chemistry Division, for creating a pleasant working atmosphere. Alberta Mok and Adele Khavari, you always be there when I need help. And the innebandy group, where I refresh every week.

Finally, I would like to give thanks to my family and my friends. Thanks for always standing by my side supporting me.

9 References

[1] Web source:

http://in.answers.yahoo.com/question/index?qid=20090120053049AADEcJ1

[2] Nazim Z. Muradov, T. Nejat Veziroglu, ”Green” path from fossil-based to hydrogen economy: An overview of carbon-neutral technologies. *International Journ. of Hydrogen Energy* 33(2008) 6804-6839

[3] Web source: http://www.ashdenawards.org/biogas

[4] Jack H. Lunsford, Catalytic conversion of methane to more useful chemicals and fuels: a challenge for the 21st century. *Catalysis Today* 63(2000) 165-174

[5] J. Haggin. Steady progress continues in Fischer–Tropsch Technology. *Chem. Eng. News*, July 23, 27–31.

[6] K. Otsuka, Y. Wang, Direct conversion of methane into oxygenates. *App. Catal. A: Gen.* 222(2001) 145-161

[7] J.J. Berzelius, *Edinburgh New Philosophical Journal*, 21(1836), 223

[8] Michael Bowker, *The basis and Applications of Heterogeneous Catalysis*, Oxford University Press 1998, p6, p8, p9

[9] Michael Bowker, *The basis and Applications of Heterogeneous Catalysis*, Oxford University Press 1998, p1-p3

[10] A. Holmen, *Catalysis Today* 142(2009) 2-8

[11] R. A. Periana, D.J. Taube, et al. A mercury- catalyzed, high-yield system for the oxidation of methane to methanol. *Science*, Vol.259, 15 Jan. 1993

[12] R.A. Periana, D.J. Taube, S. Gamble, H. Taube, T. Satoh, H. Fujii. *Science* 280(1998) 560

[13] A. Indarto, J.K. Choi, et al. Methanol synthesis over Cu and Cu-oxide-containing ZnO/Al_2O_3 using dielectric barrier discharge. *IEEE Transactions of Plasma Science*, Vol. 36, No.2, April 2008

[14] A. Indarto, D.R. Yang, et al. Partial oxidation of methane with Cu-Zn-Al catalyst in a dielectric barrier discharge. *Chemical Engineering And Process* 47(2008) 780-786

[15] Y. Yamade, A.Ueda, et al. High throughput experiments on methane partial oxidation using molecular oxygen over silica doped with various elements. *App. Catal. A: Gen.* 254(2003) 45-58

[16] X. Zhang, D. He, et al. Comparative studies on direct conversion of methane to methanol/formaldehyde over La-Co-O and ZrO_2 supported molybdenum oxide catalysts. *Topics in Catalysis* Vol. 32, Nos.3-4, Mar.2005

[17] Beata Michalkiewicz, Partial oxidation of methane to formaldehyde and methanol using molecular oxygen over Fe-ZSM-5. *App. Catal. A:Gen.* 277 (2004) 147-153

[18] K.Otsuka, Y.Wang, *App. Catal. A: Gen.* 222(2001) 145

[19] J. Lojewska, B. Zralka, et al. Promoting methane partial oxidation: homogenous additives impact on formaldehyde yield on vanadia catalyst. *Catalysis Today* 101(2005) 73-80

[20] Y.Teng, H. Sakurai, et al. Methanol formation from methane partial oxidation in CH_4-O_2-NO gaseous phase at atmospheric pressure. *App. Catal. A: Gen.* 190(2000) 283-289

[21] J.A. Barbero, M.C. Alvarez, et al. Breakthrough in the direct conversion of methane into c_1-oxygenates. *Chem. Commun.* 2008, 1184-1185

[22] O. Benlounes, S. Mansouri, et al. Direct oxidation of methane to oxygenates over heteropolyanions. *Journ. of Natural Gas* 17(2008) 309-312

[23] M. A. Banare, J. H. Cardoso, et al. Selective oxidation of methane to methanol and formaldehyde over V2O5/SiO2 catalyst. Role of NO in the gas phase. *Catalysis Letters* 56(1998) 149-153

[24] K. Otsuka, Y. Wang, Partial oxidation of methane with N_2O over $Fe_2(MoO_4)_3$ catalyst. *Catalysis Letters* 24(1994) 85-94

[25] S.H. Taylor, J.S.J. Hargreaves, et al. An initial strategy for the design of improved catalysts for methane partial oxidation. *App. Catal. A: Gen.* 126(1995) 287-296

[26] F. Li, G. Yuan, F. Yan, F. Yan, Bromine-mediated conversion of methane to C1 oxygenates over Zn-MCM-41 supported mercuric oxide. *App. Catal. A: Gen.* 335(2008) 82-87

[27] R.S. Liu, K.Y. Liew, R.E. Johnson, J.H. Lunsford, *J. Am. Chem. Soc.* 106(1984) 4117

[28] Jack H. Lunsford, Direct conversion of methane to methanol and higher hydrocarbons. *Methane Conversion* (1988) 359-371

[29] P. P. Olivera, E.M. Partito, H. Sellers, Direct synthesis of methanol over metallic catalysts. *Surface Science* 327(1995)

[30] T. J. Hall, J. S. J. Hargreaves, et al. Catalytic synthesis of methanol and formaldehyde by partial oxidation of methane. *Fuel Processing Technology* 42(1995) 151-178

[31] K. Otsuka, Y. Wang, et al. Partial oxidation of methane over iron molybdate catalyst. *Natural Gas Conversion II* (1994) 503-508

[32] G. Centi, S. Perathoner, Site isolation in iron-molybdate-based catalysts for side chain oxidation of alkylaromatics. *Topics in Catalysis* Vol. 15, No. 2-4, 2001

[33] Web Source:
http://antoine.frostburg.edu/chem/senese/101/atoms/slides/sld017.htm

[34] Y. Ding, S.-H. Yu, et al. 3D architectures of iron molybdate: phase selctive synthesis, growth mechanism, and magnetic properties. *Chem. Eur. J.* 2007, 13, 746-753

10 Appendix

10.1 Catalyst preparation recipe

Calculation:

To get 2g $Fe_2(MoO_4)_3$ theoretically, calculation is shown below:

$$n_{\mathrm{Fe2(MoO4)3}} = \frac{2g}{591.489\ g/mol} = 3.381\ mmol$$

$$n_{\mathrm{Fe}} = 2 * n_{\mathrm{Fe2(MoO4)3}} = 6.762\ mmol$$

$$Because\ \ n_{Fe(NO3)3\cdot 9H2O} = n_{\mathrm{Fe}} = 6.762\ mmol$$

$$So\quad \boldsymbol{m_{Fe(NO3)3\cdot 9H2O} = 6.672\mathrm{mmol} * 404\ g/mol = \ 2.7318\ g}$$

$$In\ reference\ 30{,}13mL\ water\ is\ used\ to\ dissolve\ 1\ mmol\ Fe(NO3)3\cdot 9H2O$$

$$water\ needed\ for\ Fe(NO3)3\ solution\text{:}\ \boldsymbol{V_{H2O} = 13\ mL * 6.762 = 87.906mL}$$

$$n_{\mathrm{Mo}} = 1.5 * n_{\mathrm{Fe}} = 10.143\ mmol$$

$$n_{\mathrm{(NH4)6Mo7O24\cdot 7H2O}} = \frac{n_{\mathrm{Mo}}}{7} = 1.449\ mmol$$

$$\boldsymbol{m_{\mathrm{(NH4)6Mo7O24\cdot 7H2O}} = 1.449\mathrm{mmol} * 1235.86\ g/mol = \ 1.7908\ g}$$

$$Same\ amount\ of\ water\ needed\ for\ \mathrm{(NH4)6Mo7O24}\ solution\text{:}\ \boldsymbol{V_{H2O} = 87.906mL}$$